

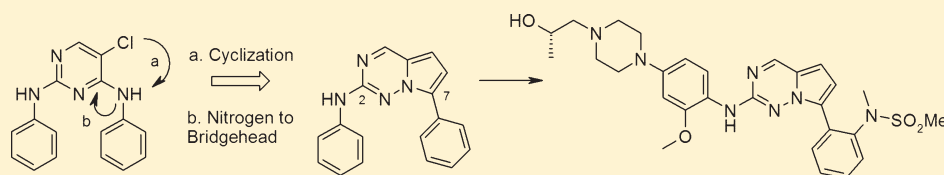
2,7-Disubstituted-pyrrolo[2,1-*f*][1,2,4]triazines: New Variant of an Old Template and Application to the Discovery of Anaplastic Lymphoma Kinase (ALK) Inhibitors with in Vivo Antitumor Activity

Gregory R. Ott,* Gregory J. Wells, Tho V. Thieu, Matthew R. Quail, Joseph G. Lisko, Eugen F. Mesaros, Diane E. Gingrich, Arup K. Ghose, Weihua Wan, Lihui Lu, Mangeng Cheng, Mark S. Albom, Thelma S. Angeles, Zeqi Huang, Lisa D. Aimone, Mark A. Ator, Bruce A. Ruggeri, and Bruce D. Dorsey

Worldwide Discovery Research, Cephalon, Inc., 145 Brandywine Parkway, West Chester, Pennsylvania 19380, United States

S Supporting Information

ABSTRACT:



A novel 2,7-disubstituted-pyrrolo[2,1-*f*][1,2,4]triazine scaffold has been designed as a new kinase inhibitor platform mimicking the bioactive conformation of the well-known diaminopyrimidine motif. The design, synthesis, and validation of this new pyrrolo[2,1-*f*][1,2,4]triazine scaffold will be described for inhibitors of anaplastic lymphoma kinase (ALK). Importantly, incorporation of appropriate potency and selectivity determinants has led to the discovery of several advanced leads that were orally efficacious in animal models of anaplastic large cell lymphoma (ALCL). A lead inhibitor (**30**) displaying superior efficacy was identified and in depth in vitro/in vivo characterization will be presented.

INTRODUCTION

Chromosomal translocations occur frequently in a select group of human cancers, including most lymphomas, leukemia, and sarcomas.¹ Individual translocations have shown a high degree of specificity for particular cancer types, and the presence of a particular translocation often correlates well with clinical behavior and outcome for specific types of cancer. Consequently, therapies directed at targets created by tumor-specific genetic aberrations may be more effective and less toxic than conventional chemotherapy. This has been best illustrated by imatinib, a small-molecule inhibitor of the fusion protein kinase BCR-ABL, which has been successfully used in the treatment of chronic myeloid leukemia (CML) associated with BCR-ABL mutations.^{2,3}

Anaplastic large cell lymphoma (ALCL) is associated with a t(2;5) (p23;q35) chromosome translocation in about 60% of cases.^{4,5} The t(2;5) translocation contains the N-terminal portion of the nucleophosmin (NPM) gene, fused to the catalytic domain of anaplastic lymphoma kinase (ALK) gene. The NPM-ALK fusion gene encodes for an 80 kDa NPM-ALK chimeric oncoprotein with constitutively active ALK tyrosine kinase activity, which plays a key role in lymphomagenesis by aberrant phosphorylation of intracellular substrates.^{5,6} The constitutively active ALK fusion protein is directly implicated in the pathogenesis of ALCL, and inhibition of ALK could markedly impair the growth of ALK-positive lymphoma cells.^{6–12} The proclivity of ALK to form gene fusions is evident from the

findings in non-small-cell lung cancer (NSCLC) cells, where a fused protein comprised of portions of the echinoderm microtubule-associated protein-like 4 (EML4) gene and the ALK gene was identified.^{13–15} The EML4-ALK fusion transcript was detected in approximately 3–7% of NSCLC patients examined, and these types of cancers were characterized with onset at a younger age and no or rare mutations in EGFR, KRAS, and TP53, all in agreement with the prevalence in non- or light smokers.^{16–18} The EML4-ALK fusion protein demonstrated oncogenic transforming activity when overexpressed in mouse fibroblasts and when tumor cells expressing EML4-ALK were inoculated in nude mice. Transgenic mice expressing EML4-ALK, specifically in lung alveolar epithelial cells, developed hundreds of adenocarcinoma nodules in both lungs within a few weeks of birth with the tumors undergoing progressive enlargement.¹⁹ These data together reinforce the pivotal role of EML4-ALK in the pathogenesis of NSCLC. Recently, various mutations of the ALK gene have been implicated in both familial and sporadic cases of neuroblastoma.^{20–23} ALK mutations in neuroblastoma cells resulted in constitutive ALK phosphorylation and attenuation or inhibition of ALK by siRNA and small-molecule ALK inhibitors resulted in profound growth inhibition in those cell lines. Altogether, these data identify ALK as a critical player in neuroblastoma development

Received: June 13, 2011

Published: August 22, 2011

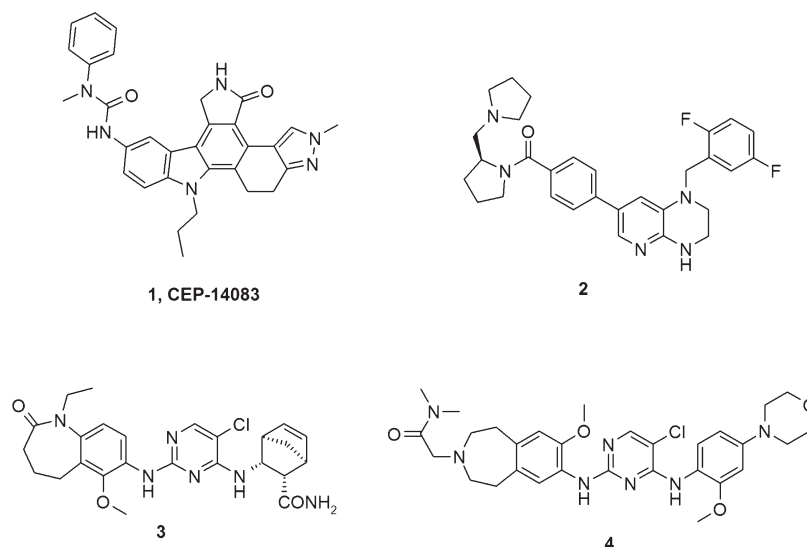


Figure 1. Small-molecule ALK inhibitors.

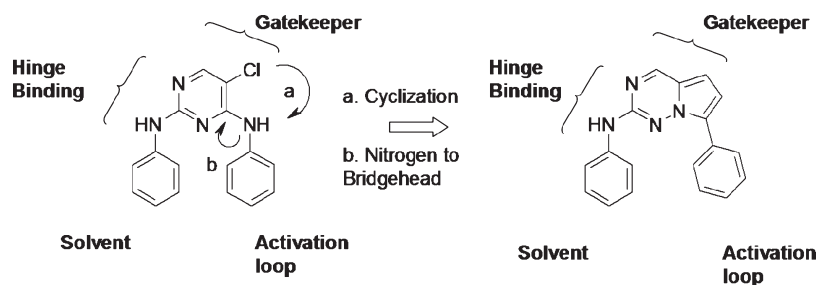


Figure 2. 6,5-Fused-bicyclic variant of diaminopyrimidine: 2,7-disubstituted-pyrrolo[2,1-*f*][1,2,4]triazines.

and suggest ALK may hence represent a very attractive therapeutic target in this disease.

Upon the basis of the clear disease linkage, ALK has emerged as an exciting target and a small-molecule inhibitor has the potential to profoundly impact ALK-driven cancers. Indeed, early clinical results for crizotinib, a dual ALK/cMet kinase inhibitor in the aminopyridine class, in patients harboring the EML4-ALK mutations in NSCLC, have been highly favorable.²⁴ Thus, small-molecule ALK inhibitors have garnered interest and a diverse set of pharmacophores have been reported including pyridone,²⁵ diaminopyrimidine,¹¹ 1*H*-pyrrolo[2,3-*d*]pyrimidine,²⁶ 1,4,5,6-tetrahydropyrrolo[3,4-*c*]pyrazole,²⁷ diaminotriazoles,²⁸ and 6,6-dimethyl-11-oxo-5*H*-benzo[*b*]carbazole-3-carbonitrile.^{29–31} Recently, we have reported small-molecule ALK inhibitors (Figure 1) within the indolocarbazole (**1**),¹⁰ tetrahydropyrido[2,3-*b*]pyrazine (**2**),³² and uniquely decorated diaminopyrimidine series (**3**, **4**).^{33,34}

CHEMISTRY

With a strong knowledge base as to potency and selectivity determinants as well as pharmaceutical/physiochemical properties within the diaminopyrimidine class of kinase inhibitors, we felt that we could take advantage of the active site conformation of this pharmacophore to further diversify the chemical space by constraining the core structure and orienting the side chains into bioactive trajectories. Shown in Figure 2 is a

general representation of the diaminopyrimidine motif in an ATP-active site of a kinase. The interactions of significance include the bidentate hydrogen-bonding of the aniline NH and the pyrimidine nitrogen to the hinge region. The diaminopyrimidine adopts an inverted “U”-shape conformation, displaying the aryl residues toward solvent and back toward the activation loop/salt-bridge region. A favorable lipophilic interaction exists with the gatekeeper residue; for ALK, the gatekeeper is leucine. To constrain the next-generation inhibitor into the bioactive conformation (Figure 2), we proposed replacing the chlorine residue with a carbon linker, favoring the lipophilic interaction with the gatekeeper region, cyclizing back onto the nitrogen of the aryl ring. Furthermore, replacing the nitrogen for a carbon and moving the nitrogen to the bridgehead position provides a unique 2,7-disubstituted-pyrrolo[2,1-*f*][1,2,4]triazine ring system.³⁵

At the time of this work, there were no published crystal structures of ALK and the original pyrrolotriazine prototypes were modeled into an homology model built from the highly homologous IGF-1R kinase using Schrodinger/Prime. IGF-1R had the maximum sequence identity/similarity with ALK.³⁶ Recently, ALK crystal structures were released (PDB ID: 2XB7²⁷ and 3LCT),³⁷ except for the flexible activation loop area, this model was very close to the reported structure. With structures now available for modeling, comparison of the cocrystal structure of a diaminopyrimidine (NVP-TAE684) and docking of pyrrolotriazine (**24**) into 2XB7 is shown in Figure 3. The

docking experiments demonstrate the expected binding mode with bidentate coordination of the pyrrolotriazine N3 to the

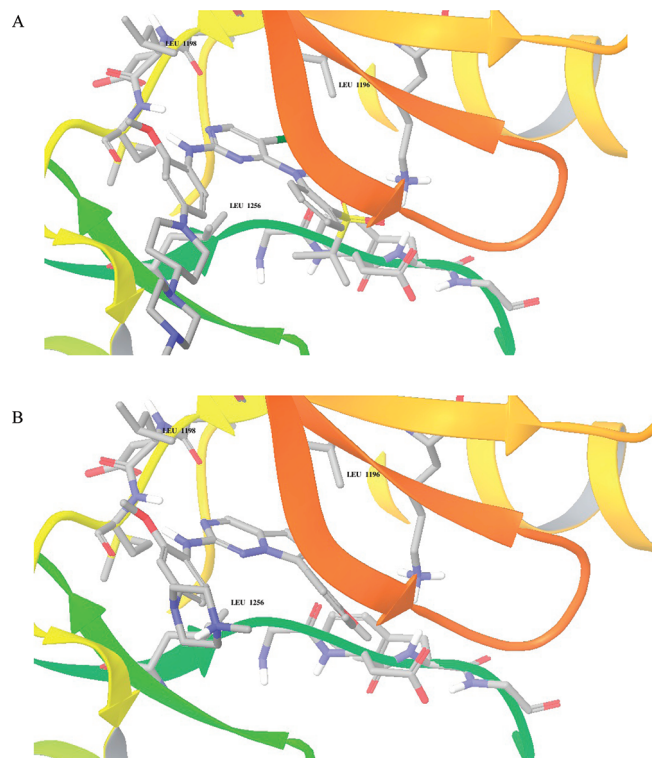


Figure 3. Comparison of the crystal structure of diaminopyrimidine NVP-TAE684 (A) and docking of 2,7-pyrrolo[2,1-f][1,2,4]triazine **24** (B).

gatekeeper+1 NH residue and aniline NH to the gatekeeper+2 carbonyl residue. The aniline fragment is disposed toward solvent, and the C5 of the pyrrolotriazine is directed toward the gatekeeper region. Furthermore, docking of **24** into the ATP bound-structure (PDB ID: 3LCT) demonstrated a comparable pose (see Supporting Information). Because of potential complications in regulating glucose homeostasis associated with inhibiting the highly homologous insulin receptor (IR) kinase, the pyrrolotriazines were docked into available structures for IR (PDB ID: 3BU6) as well as IGF-1R (PDB ID: 3QQU) to determine if there were obvious structural features to exploit or explain observed selectivities. Toward this end, docking studies showed a similar binding mode was achieved (see Supporting Information). Close examination of the sequence homology in the active site indicated the major differences between ALK/IR/IGF-1R include the gatekeeper residue. For ALK, Leu (1196) is the gatekeeper while IGF-1R and IR have Met (1076 for both). Although the conformational flexibility of Met may allow some variation in ligand acceptance, both Leu and Met are large hydrophobic residues, although Met is more polarized. Of note, however, Leu to Met mutations of the gatekeeper have been identified in a crizotinib resistant EML-ALK-positive NSCLC patient.³⁸ Furthermore, in vitro experiments with EML4-ALK and NPM-ALK Leu to Met gatekeeper changes render those enzymes resistant to ALK inhibitors.^{36,38} The gatekeeper+2 residue has also been postulated to impact overall kinome selectivity which is Leu for ALK (1198), IR (1078), and IGF-1R (1078) and Phe or Tyr for most kinases; the *o*-methoxy on the 2-*N*-aryl substituent is accommodated with Leu in the gatekeeper+2 position and thus is purported to impart selectivity. Focusing on other residue differences in the active site between ALK, IR and IGF-1R, at the bottom of the pocket, ALK

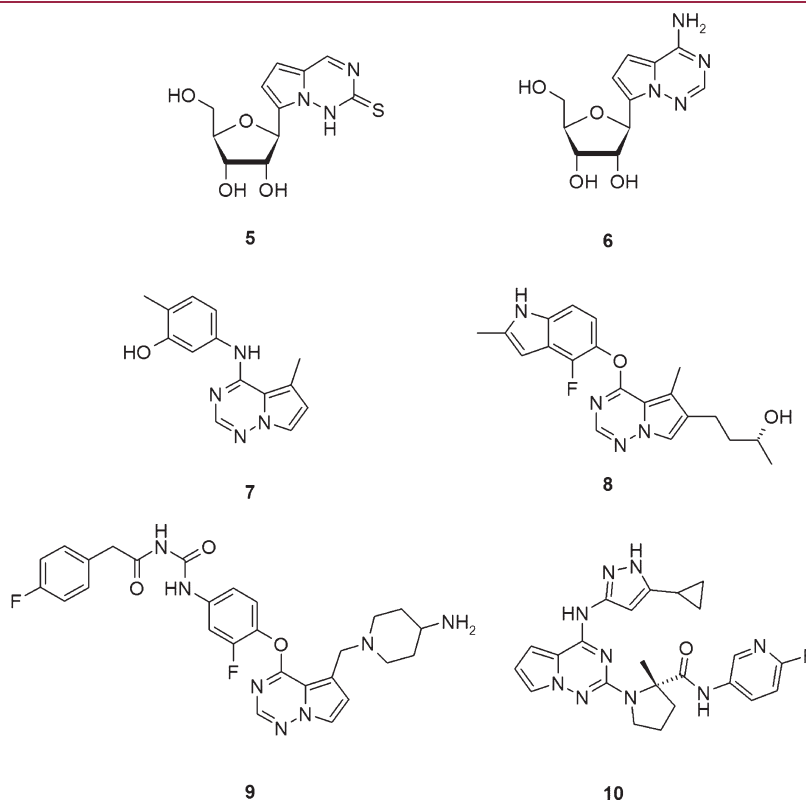
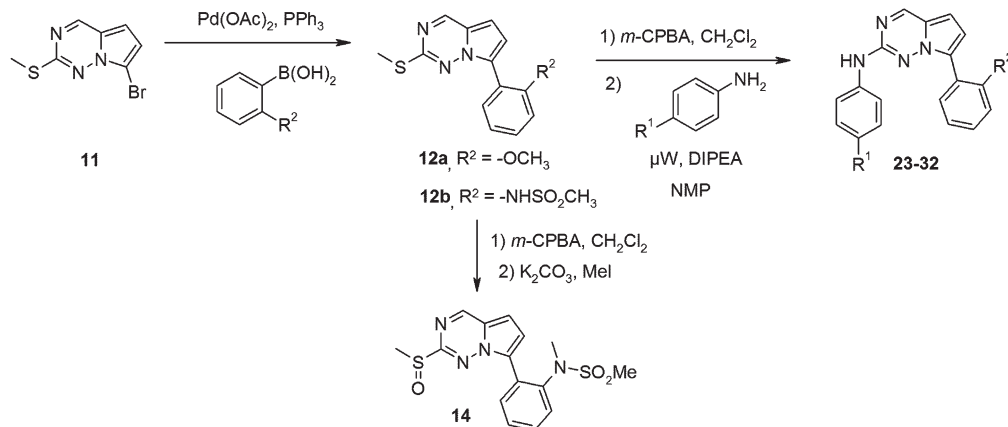


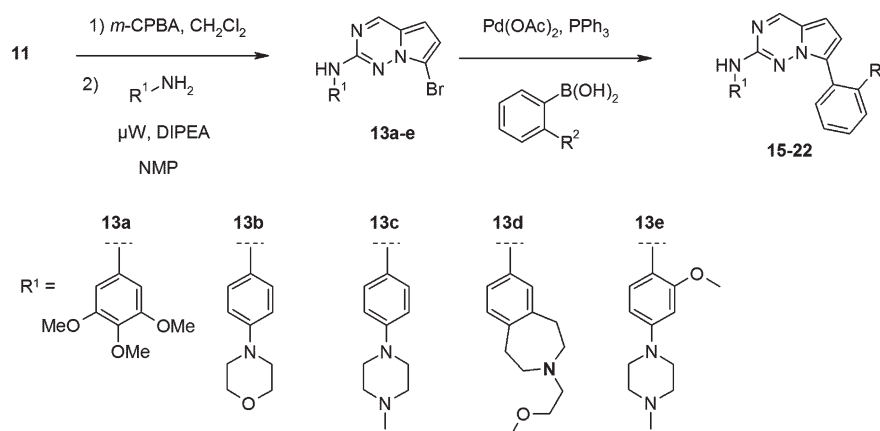
Figure 4. Pyrrolo[2,1-f][1,2,4]triazines exemplified in the medicinal chemistry literature.

Scheme 1. Synthesis from 2,7-Orthogonally Functionalized Common Intermediate

Method A



Method B



contains another Leu (1256) while IR and IGF-1R contain Met (1139), which again may impact ligand accommodation within the active site.

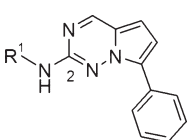
The pyrrolotriazine scaffold was introduced to the medicinal chemistry literature as a novel adenine mimic in C-linked nucleosides (**5–6**, Figure 4).^{39,40} Medicinal chemistry research surrounding this novel bridgehead nitrogen heterocycle remained relatively undeveloped until researchers at Bristol-Myers Squibb introduced 4-substituted variants as novel quinazoline mimics in the ATP-competitive kinase inhibitor field (**7**).⁴¹ The impact of this unique modification is evident by the numerous clinical candidates and array of kinase targets including VEGFR-2 (**8**)⁴² and cMet (**9**).⁴³ More recently, the pyrrolotriazine nucleus has been exploited as platform for p38 α MAP kinase inhibitors as well as 2,4-disubstituted species that utilize an aminopyrazole hinge-binding motif at the 4-position as IGF1-R kinase inhibitors (**10**).⁴⁴ The approach described herein differs significantly from these other approaches in that it capitalizes on the use of the 2,7-disubstituted-pyrrolotriazine as a constrained diaminopyrimidine, which to the best of our knowledge is a unique application of this template based upon searches of the available patent and primary literature.

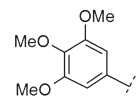
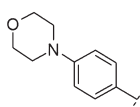
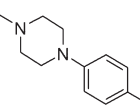
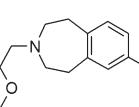
The synthesis of the target 2-anilino-7-aryl-pyrrolo[2,1-f]-[1,2,4]triazines from the orthogonally substituted common

intermediate **11**⁴⁵ in which the 2- and 7-positions may be alternately modified is shown in Scheme 1. Compound **11** could be reacted at the 7-position via Suzuki coupling to generate **12** (method A), followed by oxidation to the sulfoxide and displacement with a requisite aniline to give targets. Alternatively, oxidation to the sulfoxide and subsequent aniline displacement to give **13** (method B), followed by Suzuki coupling, could be performed to give targets.

RESULTS AND DISCUSSION

The initial series of anilines were synthesized with a simple phenyl ring in the C7 position to assess whether the pyrrolotriazine nucleus would function effectively as a pharmacophore mimic of the diaminopyrimidine scaffold. This small set was evaluated against ALK and against the highly homologous insulin receptor (IR) kinase as a counterscreen (Table 1) because inhibition of IR has been implicated in fluctuation of glucose homeostasis in preclinical animal studies.⁴⁶ Importantly, these results served to validate the 2-anilino-7-aryl-pyrrolotriazine as a kinase inhibitor platform and provided demonstrable structure–activity relationships (SAR). Analogue **15** containing the 3,4,5-trimethoxyaniline yielded an ALK IC_{50} value of 212 nM and near equipotent activity against

Table 1. SAR of the 2-Position with 7-Phenyl-pyrrolo[2,1-*f*][1,2,4]triazine


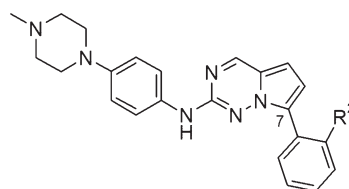
Cpd	R ¹	ALK IC ₅₀ (nM) ^a	IR IC ₅₀ (nM) ^a
15		212 ± 70	295 ± 95
16		>2000	194 ± 45
17		48 ± 8	35 ± 3
18		38 ± 11	19 ± 6

^aIC₅₀ values ± SD are reported as the average of ≥ 3 determinations

IR. The 4-morpholinophenyl derivative **16** resulted in a >9-fold loss in ALK activity, although interestingly IR activity was retained. Basic derivatives **17** (*N*-methyl piperazinylphenyl) and **18** (methoxyethyl-tetrahydrobenzazepine) proved more active; IR activity for these examples roughly paralleled ALK activity.

Having demonstrated clear SAR with the aniline fragment, we turned our attention toward the derivatization of the C7 aryl moiety (Table 2) using the 4-(*N*-methylpiperazinyl)aniline at the C2 position. Following trends associated with improving both potency and selectivity on the diaminopyrimidine core, we focused our efforts on the 2-position of the pendant aryl ring with emphasis on groups containing hydrogen bond acceptors. The introduction of the 2-methoxy group (**19**) provided a >2-fold boost to ALK enzymatic activity as compared to **17** as well as modest separation (6-fold) from IR. Interestingly, the introduction of the 2-carboxamide (**20**) or the 2-sulfonylmethyl (**21**), both effective motifs on the diaminopyrimidine scaffold, diminished activity. We surmised that the interaction of the C=O or S=O and the C6 of the pyrrolotriazine resulted in an unfavorable conformation of the ligand; this steric clash is not present in the dianilinopyrimidine variants. Again, taking a cue from the diaminopyrimidine knowledge base,⁴⁷ we introduced an *N*-linked methylsulfonamide (**22**), which regained some of the activity (ALK IC₅₀ = 260 nM). Interestingly, *N*-methylation (**23**) resulted in further improvements to both potency and IR selectivity. As compared to **19**, ALK activity improved 2- to 3-fold and IR selectivity improved by 9-fold.

At this juncture, modulation of both potency against ALK and selectivity against the insulin receptor kinase could be achieved. Furthermore, an acceptable synthetic route to diversify both the C2 and C7 positions of the pyrrolotriazine core had been

Table 2. SAR of the 2-Aryl-phenyl Group at C7


compd	R ²	ALK IC ₅₀ (nM) ^a	IR IC ₅₀ (nM) ^a
19	–OCH ₃	20 ± 2	123 ± 37
20	–C(O)NH ₂	726 ± 113	326 ± 102
21	–SO ₂ CH ₃	883 ± 233	>2000
22	–NHSO ₂ CH ₃	260 ± 57	1874 ± 485
23	–N(Me)SO ₂ CH ₃	7 ± 2	366 ± 143

^aIC₅₀ values ± SD are reported as the average of ≥ 3 determinations,

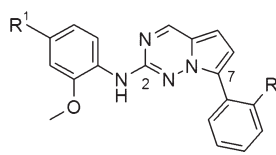
Table 3. In Vitro Profiles of **19** and **23**

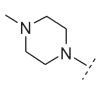
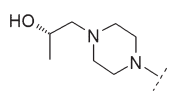
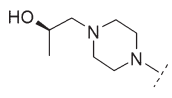
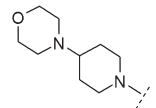
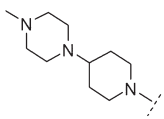
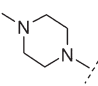
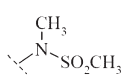
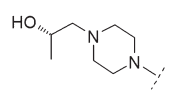
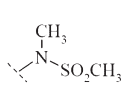
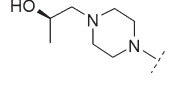
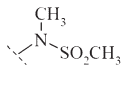
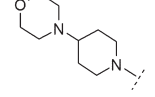
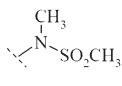
compd	liver microsome <i>t</i> _{1/2} (min) mouse, rat, human	CYP inhibition IC ₅₀ (μM) 1A2, 2C9, 2C19, 2D6, 3A4	KINOMEscan	
			<i>S</i> (90) @ 1 μM	<i>F</i> (%) (rat)
19	8, 14, 40	>30, >30, >30, >30, 9.4	0.524	4
23	30, 21, 40	>30, >30, >30, >30, 14.6	0.614	

developed. To further assess potential pharmaceutical and off-target liabilities, compounds **19** and **23** were profiled for in vitro liver microsome stability, cytochrome P450 (CYP) isozyme activity, and broader kinase selectivity; **19** was also profiled for cellular activity and pharmacokinetics in rat (Table 3). The CYP inhibition profile was quite favorable and in vitro metabolic stability was reasonable for these early stage inhibitors. However, both inhibitors demonstrated broad interaction against an array of kinase targets as exemplified by the high *S*(90)⁴⁸ value when screened at 1 μM in the Ambit KINOMEscan. Importantly, **19** displayed an IC₅₀ value of 100 nM for inhibition of NPM-ALK phosphorylation in Karpas-299 cells. The rat pharmacokinetics were modest with **19** demonstrating a short iv half-life (*t*_{1/2} = 0.5 h), iv clearance of 60 mL/min/kg, which is slightly higher than liver blood flow (50 mL/min/kg), and only 4% oral bioavailability.

The early assessment of the in vitro/in vivo drug-like properties of **19** and **23** prompted further investigation of this core, with kinase selectivity and oral bioavailability as specific areas for improvement. Notably, prior SAR had identified the 2-methoxy group on the aniline fragment as a key selectivity determinant in the dianilinopyrimidine core. Likewise, on the pyrrolotriazine core, this modification produced a positive outcome as illustrated in Table 4. **24** displayed improved enzyme and similar cell potency to **19**, and importantly, the broad interaction with the kinase decreased markedly as assessed by the *S*(90) score of 0.085 as compared to 0.524 for **19**. This modification, however, yielded no improvement to in vitro metabolic stability relative to **19** (Table 4). Targeting the *N*-methyl group on the piperazine as a potential site for dealkylative metabolism, we introduced 2-hydroxypropyl substituents (**25** and **26**) to increase sterics as well as mitigate the basicity. This modification improved in vitro stability (liver microsome *t*_{1/2} > 40 min) but only led to modest increases in

Table 4. Optimized Analogues at C2 and C7



Ex	R ¹	R ²	ALK IC ₅₀ ^a (nM)	Cell IC ₅₀ ^b (nM)	IR IC ₅₀ ^a (nM)	KINOMEScan® S(90) @ 1 μM	F% (Rat)
24		-OCH ₃	9 ± 3	100	391 ± 80	0.085	--
25		-OCH ₃	5 ± 2	100	206 ± 49	0.067	8%
26		-OCH ₃	3.8 ± 0.7	80	160 ± 36	0.067	6%
27		-OCH ₃	9 ± 3	85	357 ± 95	0.050	34%
28		-OCH ₃	8.8 ± 0.8	70	266 ± 65	0.164	38%
29			9 ± 2	200	934 ± 323	0.187	--
30			10 ± 2	60	1137 ± 398	0.187	38%
31			15 ± 5	80	1171 ± 169	0.194	41%
32			7 ± 2	50	809 ± 299	0.187	47%

^aIC₅₀ values ± SD are reported as the average of ≥3 determinations ^bIC₅₀ values are reported as a mean of at least two determinations

rat oral bioavailability ($F = 8\%$ and 6% , respectively). Again, taking a cue from the diaminopyrimidine knowledge base, extending the basic functionality and replacing the piperazine with a 4-morpholino-piperidine or an *N*-methyl-piperazinylpiperidine (**27** and **28**) maintained both enzyme and cellular potency and led to a clear improvement to oral pharmacokinetics, with oral bioavailability in rat of 34% and 38% , respectively. Surprisingly, **28** displayed broader activity against the kinase as compared to the related morpholine analogue as shown by the $S(90)$ at $1\ \mu\text{M}$. Concurrent with the 2-methoxyphenyl C7-position SAR, similar modifications were implemented on the C7 *N*-methyl-methylsulfonamide phenyl analogues. Interestingly, a broader interaction with the kinase was realized, with $S(90)$ values (screening at $1\ \mu\text{M}$) ranging from 0.187 to 0.194 , although against the insulin receptor

kinase, improved selectivity was noted. Analogue **29**, containing the *N*-methylpiperazine, displayed a drop-off in cellular activity on the cusp of our desired range ($\text{IC}_{50} < 200\ \text{nM}$). Fortunately, the hydroxypropyl derivatives **30** and **31** regained the cellular activity and, importantly, displayed acceptable oral bioavailability ($F = 38\%$ and 41% , respectively). Similarly, **32** gave acceptable potency and oral bioavailability.

At this stage, we had identified a set of ligands (**27**, **28**, **30**, **31**, **32**) with potent enzymatic and cellular activity, acceptable selectivity (against IR and the broader kinase), and favorable pharmacokinetics in rat. To differentiate these prospective candidates, single dose ($30\ \text{mg/kg}$, po) PK/PD studies in ALK-driven subcutaneous tumor xenografts (SUP-M2) were performed. Prior studies with small-molecule ATP-competitive inhibitors, both internal³³ and externally reported,¹² demonstrated

that complete/near complete ablation of signaling is required to effect a robust antitumor response. Three of the five com-

Table 5. Anti-tumor Efficacy Results with 27, 30, and 32

compd	10 mg/kg, po, bid	30 mg/kg, po, bid (% TGI)	55 mg/kg, po, bid (% TGI)
27	no significant effect	60	98
30	35% TGI ^a	81	98
32	no significant effect	50	96

^a TGI = tumor growth inhibition: calculated from tumor volume on final day relative to vehicle treated group.

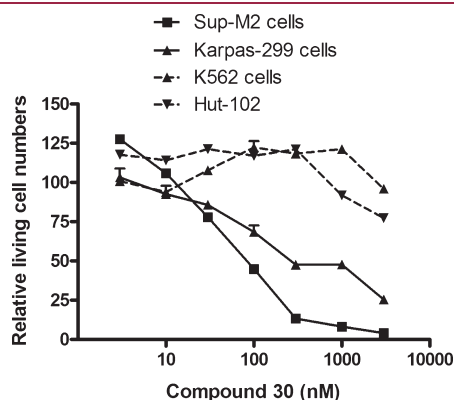


Figure 5. MTS assay in ALK-positive and ALK-negative cell lines.

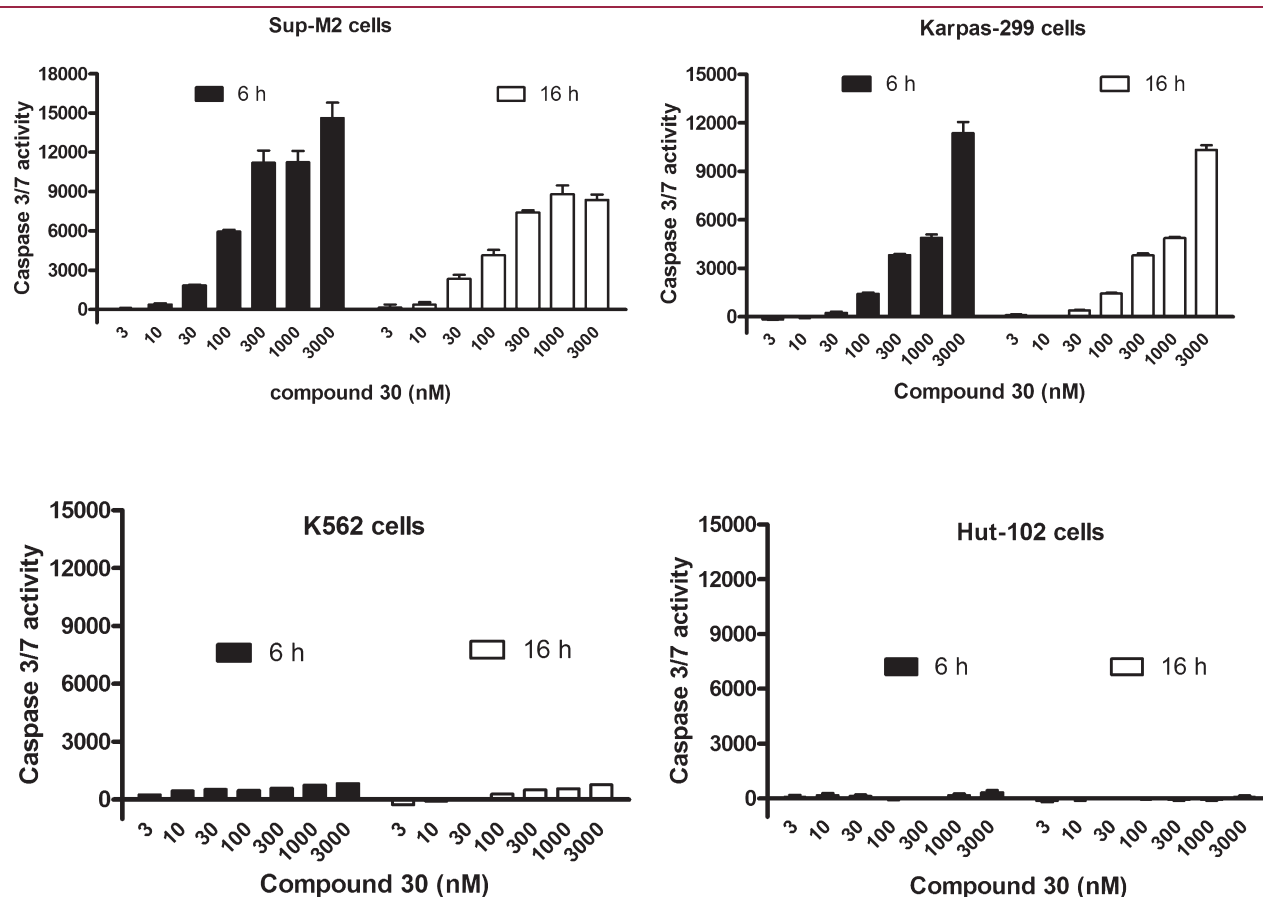


Figure 6. Caspase 3/7 induction in ALK-positive and ALK-negative cell lines.

pounds (27, 30, and 32) demonstrated sufficient target inhibition in vivo (>75% over 6–12 h) to be evaluated in chronic dosing antitumor studies. Upon the basis of the PK/PD data, with bid dosing at 30 mg/kg and higher, antitumor responses should be effected with 27, 30, and 32. Shown in Table 5 are the results of oral antitumor efficacy studies in SUP-M2 subcutaneous tumor xenografts in Scid mice of 27, 30, and 32. Importantly, all three compounds were well tolerated with no significant body-weight loss and all three demonstrated dose-dependent antitumor responses with near 100% tumor growth inhibition (TGI) and 100% of the mice in each cohort displaying tumor regressions at the highest dose (55 mg/kg, bid). Compound 30 clearly showed a better response at lower doses with 81% TGI and 87.5% of the mice displaying partial tumor regressions at 30 mg/kg bid, as well as significant tumor growth inhibition (35%) at 10 mg/kg bid (no tumor regressions), whereas 27 displayed no significant activity at 10 mg/kg bid and 60% TGI, with 62.5% of mice displaying partial regressions and 32 displaying only 50% TGI at 30 mg/kg bid.

Data presented hereafter provide in-depth characterization of in vitro and in vivo properties of the lead 30 in a variety of pharmacologic and pharmaceutic assays and support the conclusion that the specific effects of 30 are mediated by ALK inhibition and not off-target activity. The proliferation and survival of ALK-positive ALCL cells (Karpas-299 and Sup-M2) and ALK-negative cells (K562, a leukemia cell line, and Hut-102, a lymphoma cell line) in culture were evaluated by MTS and caspase 3/7 activation assays. Compound 30 displayed concentration-dependent (1–3000 nM) growth inhibition of

Karpas-299 ($IC_{50} = 477$ nM) and Sup-M2 ($IC_{50} = 87$ nM) cells in culture, with the extent of growth inhibition consistent with cellular inhibition of NPM-ALK phosphorylation in these cells (Figure 5). In contrast, **30** had minimal growth inhibition on ALK-negative K562 cells at concentrations up to 3000 nM, suggesting that at the concentrations studied, **30** exerts growth inhibition on ALK-positive ALCL cells primarily through inhibiting NPM-ALK activity.

The in vitro cytotoxicity of **30** in cells was also assessed via measurement of pro-apoptotic caspase 3/7 activity. As shown in Figure 6, treatment of Karpas-299 and Sup-M2 cell lines with **30** led to concentration-related caspase 3/7 activation. In contrast, no caspase 3/7 activation was detected in K562 or Hut-102 cells treated with **30**. These data indicate that **30** exerts in vitro cytotoxicity on ALK-positive ALCL cells mainly through inhibiting NPM-ALK activity.

Assessment of the in vitro ADME and in vitro safety pharmacology properties of **30** were also promising. In vitro metabolic stability was highly favorable with $t_{1/2} > 40$ min in mouse, rat, and human liver microsomes. Permeability in a Caco-2 assay was high with low efflux: $P_{app} (A \rightarrow B) = 20.3 \times 10^{-6}$ cm/s and a PDR < 2 . Plasma protein binding was 91% in mouse, 68% in rat, and 83% in humans. An assessment of potential cardiovascular toxicity was performed using a hERG patch clamp assay; compound **30** displayed an IC_{50} value of 9.1 μ M. Minimal inhibition of the major cytochrome P450 (CYP) isozymes 1A2, 2C9, 2C19, 2D6, and 3A was noted with an $IC_{50} > 12$ μ M for each.

Table 6. Pharmacokinetics of **30**

	PK parameters	Scid mouse ^a	rat ^b
iv	dose (mg/kg)	1	1
	$t_{1/2}$ (h)	1.0	0.8 \pm 0.2
	Cl (mL/min/kg)	24	49 \pm 8
	V_d (L/kg)	2.1	3.3 \pm 0.4
	AUC (ng·h/mL)	661	343 \pm 52
po	dose (mg/kg)	10	5
	t_{max} (h)	1	2 \pm 0
	$t_{1/2}$ (h)	1.6	ND ^c
	AUC (ng·h/mL)	2521	610 \pm 165
	F (%)	36	38 \pm 10

^aDeterminantantsof 3 mice per time point, average value. ^bDeterminants of 3 for each dosing group, average value \pm SEM. ^cND = not determined.

The full in vivo PK parameters for **30** in Scid mouse and rat are listed in Table 6. Similar iv $t_{1/2}$ values were observed with a higher clearance and volume of distribution observed in rat. Following oral dosing, a longer t_{max} was observed in rat (2 h) versus mouse (1 h). Oral bioavailability was similar for the two species (36% and 38%).

Shown in Figure 7 are the PK/PD results following a single oral dose of **30** (30 mg/kg) in vehicle (PEG400). Inhibition of NPM-ALK autophosphorylation was measured in tumor lysates from ALK-positive ALCL tumor xenografts (SUP-M2) in Scid mouse. Roughly 75% inhibition of NPM-ALK phosphorylation in tumor xenografts up to 12 h was observed with signal returning by 24 h. These results suggested with daily dosing, bid

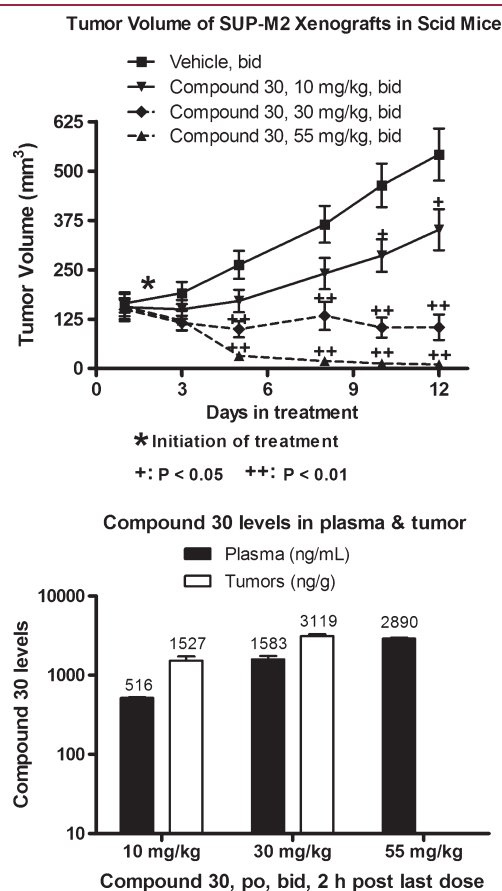


Figure 8. In vivo efficacy of **30** in ALK-positive SUP-M2 xenografts.

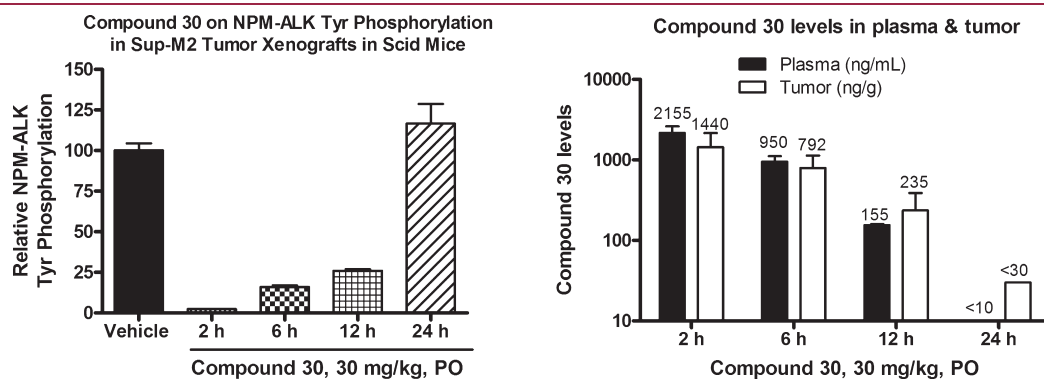


Figure 7. Single oral dose PK/PD of **30**.

at 30 mg/kg or higher, sustained target inhibition would be obtained.

Indeed, oral dosing bid with **30**, at 10, 30, and 55 mg/kg (Figure 8), resulted in dose-dependent antitumor activity (as previously noted in Table 5). Complete tumor regressions following 12 day treatment at 55 mg/kg, po, bid were observed, and all dosing regimens were well tolerated with no overt toxicity and no significant body-weight loss. Dose-related levels of **30** were found in plasma and tumor lysates collected at 2 h post final dosing (Figure 8). Relative to the single dose PK/PD study, approximately 2-fold increase in compound levels were observed in tumors with 12 days of bid dosing.

CONCLUSION

In summary, we have designed and synthesized a novel 2,7-disubstituted-pyrrolo[2,1-*f*][1,2,4]triazine scaffold as a constrained diaminopyrimidine pharmacophore mimic. Importantly, we have validated this scaffold as a new kinase inhibitor platform for designing ALK inhibitors. We were able to incorporate appropriate potency and selectivity determinants and demonstrate oral bioavailability with numerous analogues. Furthermore, we have advanced several lead candidates into in vivo efficacy studies. Compound **30** displayed a favorable overall profile with potency in enzyme and cellular systems. Selectivity against the highly homologous insulin receptor kinase was achieved as well as selective pro-apoptotic caspase induction and toxicity in ALK-driven cell lines versus non-ALK-driven cell lines. Compound **30** displayed favorable in vitro ADME properties, acceptable oral bioavailability in two species, and dose-dependent antitumor efficacy with oral dosing in ALK-positive tumor xenografts. Compound **30** advanced to late stage preclinical safety assessment studies, and the results will be reported separately.

EXPERIMENTAL SECTION

Unless otherwise indicated, all reagents and solvents were obtained from commercial sources and used as received. ^1H and ^{13}C NMRs were obtained on a Bruker Avance at 400 and 100 MHz, respectively, in the solvent indicated with tetramethylsilane as an internal standard. Analytical HPLC to assess final compound purity was run using a Zorbax RX-C8, 5 mm \times 150 mm column eluting with a mixture of acetonitrile and water containing 0.1% trifluoroacetic acid with a gradient of 10–100% over 5 min with wavelength of 254 and 290 nm; final compounds were $\geq 95\%$ purity based on Area%. LC/MS results were obtained on either of two instruments. LC/MS analysis was performed on a Waters Aquity Ultra Performance LC with a 2.1 mm \times 50 mm Waters Aquity UPLC BEH C18 1.7 μm column. The target column temperature was 45 $^\circ\text{C}$, with a run time of 2 min, a flow rate of 0.600 mL/min, and a solvent mixture of 5% (0.1% formic acid/water):95% (acetonitrile/0.1% formic acid). The mass spectrometry data was acquired on a Micromass LC-ZQ 2000 quadrupole mass spectrometer. Alternatively, LCMS analysis was performed on a Bruker Esquire 200 ion trap. High resolution mass spectrometry was performed on a Waters Synapt G2 Q-TOF mass spectrometer using leucine-enkephalin as a lock-mass standard. Automated column chromatography (SiO_2) was performed on a CombiFlash Companion (ISCO, Inc.). Melting points were taken on a Mel-Temp apparatus and are uncorrected.

General Procedure for Suzuki Coupling [Method A or B]. A solution of $\text{Pd}(\text{OAc})_2$ (92 mg, 0.41 mmol) and triphenylphosphine (269 mg, 1.02 mmol) in 1,4-dioxane was purged with nitrogen while being stirred and bromide substrate (2.0 mmol) and arylboronic acid (4.1 mmol) was added, followed by DMF (15 mL) and 1.5 M of sodium

carbonate in water (12 mL, 17 mmol). After being thoroughly purged with nitrogen, the reaction was heated at 80 $^\circ\text{C}$ for 3 h with stirring. The mixture was concentrated and the residue partitioned between EtOAc and water. The organic phase was washed with water and brine, dried (MgSO_4), filtered, concentrated, and purified by flash chromatography (SiO_2) or ISCO automated flash chromatography using gradient elution with MeOH/dichloromethane or ethyl acetate/hexane solvent systems. Alternatively, final products were isolated by preparative reverse phase HPLC eluting with water/acetonitrile gradient (0.1% TFA modifier).

General Procedure for *m*-CPBA Oxidation [Method A or B]. A solution of methylsulfanyl substrate (1.65 mmol) in dichloromethane (50 mL) was treated with 70% *m*-chloroperbenzoic acid (446.0 mg, 1.8 mmol) at room temperature and stirred for 2 h. The mixture was stirred with 10% $\text{Na}_2\text{S}_2\text{O}_3$ (25 mL) for 5 min. The organic phase was washed with saturated aqueous NaHCO_3 and brine, dried (MgSO_4), filtered, and concentrated and used without further purification.

General Procedure for Aniline $\text{S}_\text{N}\text{Ar}$ Displacement [Method A or B]. Methanesulfinyl substrate (0.348 mmol), *N,N*-diisopropylethylamine (0.1818 mL, 1.044 mmol), and aniline (0.696 mmol) were dissolved in *N*-methylpyrrolidinone (0.224 mL), and the reaction was heated in a microwave at 180 $^\circ\text{C}$ for 40 min or until HPLC showed consumption of starting material. The solvent was then evaporated under reduced pressure and the product isolated by flash chromatography (SiO_2) or ISCO automated flash chromatography using gradient elution with MeOH/dichloromethane or ethyl acetate/hexane solvent systems. Alternatively, final products were isolated by preparative reverse-phase HPLC eluting with water/acetonitrile gradient (0.1% TFA modifier).

(4-Morpholin-4-yl-phenyl)-(7-phenyl-pyrrolo[2,1-*f*][1,2,4]-triazin-2-yl)amine (16), Method B. *a.* Following the general procedure for *m*-CPBA oxidation and $\text{S}_\text{N}\text{Ar}$ displacement, **11** and 4-(4-morpholino)aniline were converted to (7-bromo-pyrrolo[2,1-*f*][1,2,4]-triazin-2-yl)-(4-morpholin-4-yl-phenyl)-amine (**13b**) and isolated as a brown solid (1.14 g, 71%). ^1H NMR ($\text{DMSO}-d_6$) δ 9.42 (s, 1H), 8.89 (s, 1H), 7.76 (d, 1H, J = 8.96 Hz), 6.82–6.98 (m, 4H), 3.73 (t, 4H, J = 4.57 Hz), 3.05 (t, 4H, J = 4.77 Hz). LC/MS (ESI^+) m/z 374.09 ($\text{M} + \text{H}$) $^+$.

b. Following the general procedure for Suzuki coupling, **13b** and phenylboronic acid were converted to (4-morpholin-4-yl-phenyl)-(7-phenyl-pyrrolo[2,1-*f*][1,2,4]-triazin-2-yl)amine (**16**) and isolated as a yellow solid (78 mg, 45%); mp 219–220 $^\circ\text{C}$. ^1H NMR ($\text{DMSO}-d_6$) δ 8.68 (s, 1H), 8.14 (d, 1H, J = 7.42 Hz), 7.58 (d, 1H, J = 8.78 Hz), 7.49 (t, 1H, J = 7.57 Hz), 6.99 (d, 1H, J = 4.72 Hz), 6.92 (d, 2H, J = 9.12 Hz), 6.82 (d, 1H, J = 5.32 Hz), 6.68 (broad s, 1H), 3.88 (t, 4H, J = 4.68 Hz), 3.13 (t, 4H, J = 4.64 Hz). LC/MS (ESI^+) m/z 372.2 ($\text{M} + \text{H}$) $^+$. HPLC 95 Area%.

[4-(4-Methyl-piperazin-1-yl)-phenyl]-(7-phenyl-pyrrolo[2,1-*f*][1,2,4]-triazin-2-yl)-amine (17) [Method B]. *a.* Following the general procedure for *m*-CPBA oxidation and $\text{S}_\text{N}\text{Ar}$ displacement, **11** and 4-(4-methyl-piperazin-1-yl)-phenylamine were converted to 7-bromo-pyrrolo[2,1-*f*][1,2,4]-triazin-2-yl-[4-(4-methyl-piperazin-1-yl)-phenyl]-amine (**13c**) as a yellow solid (220 mg, 49%). ^1H NMR ($\text{DMSO}-d_6$) δ 9.40 (s, 1H), 8.85 (s, 1H), 7.75 (d, J = 8.97 Hz, 2H), 6.88–6.98 (m, 4H), 3.02–3.07 (broad s, 4H), 2.37–2.247 (broad s, 4H), 2.21 (s, 3H).

b. Following the general procedure for Suzuki coupling, **13c** and phenylboronic acid were converted to [4-(4-methyl-piperazin-1-yl)-phenyl]-(7-phenyl-pyrrolo[2,1-*f*][1,2,4]-triazin-2-yl)-amine (**17**), yellow solid (18 mg, 29%); mp 246–248 $^\circ\text{C}$. ^1H NMR ($\text{DMSO}-d_6$) δ 9.22 (s, 1H), 8.23 (s, 1H), 8.19 (d, J = 8.40 Hz, 2H), 7.63 (d, J = 9.05 Hz, 2H), 7.53 (t, J = 7.88 Hz, 2H), 7.38 (t, J = 7.40 Hz, 1H), 7.15 (d, J = 4.72 Hz, 1H), 6.85–6.95 (m, 3H), 3.10–3.17 (m, 4H), 2.42–2.60 (m, 4H), 2.27 (s, 3H). LC/MS (ESI^+) m/z 385.28 ($\text{M} + \text{H}$) $^+$. HPLC 96 Area%.

[3-(2-Methoxy-ethyl)-2,3,4,5-tetrahydro-1H-benzo[*d*]azepin-7-yl]-(7-phenyl-pyrrolo[2,1-*f*][1,2,4]-triazin-2-yl)-amine (18) [Method B]. *a.* Following the general procedure for *m*-CPBA

oxidation and S_NAr displacement, **11** and 3-(2-methoxy-ethyl)-2,3,4,5-tetrahydro-1H-benzo[d]azepin-7-ylamine were converted to (7-bromopyrrolo[2,1-f][1,2,4]triazin-2-yl)-[3-(2-methoxy-ethyl)-2,3,4,5-tetrahydro-1H-benzo[d]azepin-7-yl]-amine (**13d**) as a yellow solid (130 mg, 62%). 1H NMR ($CDCl_3$) δ 8.57 (s, 1H), 7.54 (s, 1H), 7.48 (dd, J = 1.96, 6.04 Hz, 1H), 7.69 (s, 1H), 7.09 (d, J = 8.04 Hz, 1H), 6.93 (s, 1H), 6.78 (d, J = 4.72 Hz, 1H), 6.73 (d, J = 4.72 Hz, 1H), 3.54 (t, J = 5.68 Hz, 2H), 3.36 (s, 3H), 2.65–3.00 (m, 10H).

b. Following the general procedure for Suzuki coupling, **13d** and phenylboronic acid were converted to **18** as a yellow solid (48 mg, 37% yield); mp 116–118 °C. 1H NMR ($DMSO-d_6$) δ 9.36 (s, 1H), 8.96 (s, 1H), 8.11 (d, J = 7.57 Hz, 1H), 7.69 (s, 1H), 7.51 (t, J = 7.48 Hz, 2H), 7.41 (t, J = 7.28 Hz, 1H), 7.34 (d, J = 8.04 Hz, 1H), 7.17 (d, J = 4.72 Hz, 1H), 7.02 (d, J = 8.16 Hz, 1H), 6.94 (d, J = 4.72 Hz, 1H), 3.46 (t, J = 5.80 Hz, 2H), 3.24 (s, 3H), 2.79 (broad s, 4H), 2.50–2.70 (m, 6H). HPLC: 95 Area%. LC/MS (ESI^+) m/z 414.26 ($M + H$) $^+$.

[7-(2-Methoxy-phenyl)pyrrolo[2,1-f][1,2,4]triazin-2-yl]-[4-(4-methyl-piperazin-1-yl)-phenyl]amine (**19**) [Method B]. Following the general procedure for Suzuki coupling, **13c** and 2-methoxyphenylboronic acid were converted to **19** (38 mg, 46%) as a yellow solid; mp 199–200 °C. 1H NMR ($DMSO-d_6$) δ 9.12 (s, 1H), 8.89 (s, 1H), 7.81 (d, J = 7.77 Hz, 1H), 7.56 (d, J = 8.93 Hz, 2H), 7.45 (t, J = 7.44 Hz, 1H), 7.21 (d, J = 8.28 Hz, 1H), 7.12 (t, J = 7.53 Hz, 1H), 6.91 (t, J = 4.56 Hz, 1H), 6.88 (d, J = 4.61 Hz, 1H), 6.79 (d, J = 8.92 Hz, 2H), 3.79 (s, 3H), 2.97–3.10 (broad m, 4H), 2.42–2.53 (broad m, 4H), 2.22 (s, 3H). HPLC: 99 Area%. LC/MS (ESI^+) m/z 415.21 ($M + H$) $^+$.

2-[2-[4-(4-Methyl-piperazin-1-yl)-phenylamino]-pyrrolo[2,1-f][1,2,4]triazin-7-yl]-benzamide (**20**) [Method B]. Following the general procedure for Suzuki coupling, **13c** and 2-aminocarbonylphenylboronic acid were converted to **20** (52.56 mg, 48% yield) as a lyophilized yellow powder. 1H NMR ($DMSO-d_6$) δ 9.13 (s, 1H), 8.90 (s, 1H), 7.94 (d, J = 7.80 Hz, 1H), 7.66 (m, 1H), 7.57 (m, 4H), 7.49 (m, 1H), 7.31 (m, 1H), 6.84 (m, 4H), 3.02 (m, 4H), 2.44 (m, 4H), 2.21 (s, 3H). HPLC: >95 Area%. LC/MS (ESI^+) m/z 428.2 ($M + H$) $^+$.

[7-(2-Methanesulfonyl-phenyl)-pyrrolo[2,1-f][1,2,4]triazin-2-yl]-[4-(4-methyl-piperazin-1-yl)-phenyl]-amine (**21**) [Method B]. Following the general procedure for Suzuki coupling, **13c** and 2-(methylsulfonyl)phenylboronic acid were converted to **21** (28.19 mg, 24% yield) as a yellow lyophilized powder. 1H NMR ($DMSO-d_6$) δ 9.17 (s, 1H), 8.96 (s, 1H), 8.17 (d, J = 7.88 Hz, 1H), 7.90 (m, 1H), 7.79 (m, 1H), 7.73 (m, 1H), 7.33 (d, J = 7.97 Hz, 2H), 6.93 (dd, J = 3.68, 9.97 Hz, 2H), 6.67 (d, J = 7.96 Hz, 2H), 2.98 (m, 4H), 2.86 (s, 3H), 2.42 (m, 4H), 2.20 (s, 3H). HPLC: >95 Area%. LC/MS (ESI^+) m/z 463.2 ($M + H$) $^+$.

N-[2-[2-[4-(4-Methyl-piperazin-1-yl)-phenylamino]-pyrrolo[2,1-f][1,2,4]triazin-7-yl]-phenyl]-methanesulfonamide TFA Salt (**22**) [Method A]. a. Following the general procedure for Suzuki coupling, **11** (500 mg, 2.0 mmol) and 3-methylsulfonyl-aminophenyl boronic acid (881 mg, 4.10 mmol) were converted to **12b** (560 mg, 84% yield). 1H NMR ($DMSO-d_6$) δ 9.03 (s, 1H), 8.88 (s, 1H), 7.67–7.65 (m, 1H), 7.56–7.45 (m, 2H), 7.38–7.34 (m, 1H), 7.16 (d, J = 4.7 Hz, 1H), 7.11 (d, J = 4.7 Hz, 1H), 2.81 (s, 3H), 2.43 (s, 3H). LC/MS (ESI^+) m/z 335 ($M + H$) $^+$.

b. Following the general procedure for *m*-CPBA oxidation, **12b** was converted to N-[2-(2-methanesulfinylpyrrolo[2,1-f][1,2,4]triazin-7-yl)-phenyl]-methanesulfonamide as a yellow solid and [LC/MS (ESI^-) m/z 349 ($M - H$) $^-$] used without further purification following the general procedure for S_NAr displacement with 4-(4-methyl-piperazin-1-yl)-phenylamine to afford **22** (36.23 mg, 27% yield) as a lyophilized powder. 1H NMR ($DMSO-d_6$) δ 9.37 (s, 1H), 8.98 (s, 1H), 8.82 (s, 1H), 7.72 (d, J = 6.81 Hz, 1H), 7.53 (m, 4H), 7.43 (m, 1H), 6.97 (d, J = 4.64 Hz, 1H), 6.93 (d, J = 4.60 Hz, 1H), 6.87 (d, J = 9.08 Hz, 2H), 3.70 (m, 2H), 3.51 (m, 2H), 3.15 (m, 2H), 2.86 (m, 5H), 2.67 (s, 3H). LC/MS (ESI^+) m/z 478.1 ($M + H$) $^+$. HPLC: >95 Area%.

N-Methyl-N-[2-[2-[4-(4-methyl-piperazin-1-yl)phenylamino]-pyrrolo[2,1-f][1,2,4]triazin-7-yl]-phenyl]methanesulfonamide TFA Salt (**23**) [Method A]. a. Following the general procedure for *m*-CPBA oxidation, **12b** was converted to N-[2-(2-methanesulfinylpyrrolo[2,1-f][1,2,4]triazin-7-yl)-phenyl]-methanesulfonamide and used without further purification.

b. To N-[2-(2-Methanesulfinylpyrrolo[2,1-f][1,2,4]triazin-7-yl)-phenyl]-methanesulfonamide (600.0 mg, 1.71 mmol) and potassium carbonate (946.6 mg, 6.85 mmol) in *N,N*-dimethylformamide (25 mL) was added methyl iodide (0.31 mL, 5.14 mmol). The mixture was stirred at room temperature overnight. The mixture was concentrated and the residue partitioned between dichloromethane and water. The organic phase was washed with brine, dried ($MgSO_4$), filtered, and concentrated. Flash chromatography (ISCO, 5% MeOH/dichloromethane) gave **14** as a yellow solid (548 mg, 76%). 1H NMR ($DMSO-d_6$) δ 9.03 (s, 1H), 7.75–7.71 (m, 2H), 7.64, 7.60 (m, 1H), 7.57–7.52 (m, 1H), 7.32 (s, 2H), 3.27 (s, 3H), 2.92 (s, 3H), 2.77 (s, 3H). LCMS (ESI^+) m/z 365.05 ($M + H$) $^+$.

c. Following the general procedure for S_NAr displacement, **14** and 4-(4-methyl-piperazin-1-yl)phenylamine were reacted to give **23** isolated as a trifluoroacetic acid salt orange lyophilate (105.2 mg, 58% yield). 1H NMR ($DMSO-d_6$) δ 9.57 (s, 1H), 9.24 (s, 1H), 8.94 (s, 1H), 8.01 (d, J = 7.6 Hz, 1H), 7.56 (m, 4H), 6.97 (s, 1H), 6.93 (s, 1H), 6.87 (d, J = 7.6 Hz, 2H), 3.71 (d, J = 13.0 Hz, 2H), 3.5 (d, J = 12.0 Hz, 2H), 3.16 (m, 2H), 3.08 (s, 3H), 2.89 (s, 3H), 2.86 (m, 5H). LCMS (ESI^+) m/z 492 ($M + H$) $^+$. HPLC: 95 Area%.

[2-Methoxy-4-(4-methyl-piperazin-1-yl)-phenyl]-[7-(2-methoxy-phenyl)-pyrrolo[2,1-f][1,2,4]triazin-2-yl]-amine (**24**) [Method B]. a. Following the general procedure for S_NAr displacement, 2-methoxy-4-(4-methyl-piperazin-1-yl)-phenylamine (1.08 g, 4.90 mol) and 7-bromo-2-methanesulfinylpyrrolo[2,1-f][1,2,4]triazine (580 mg, 2.23 mol) were converted to **13e** as a yellow solid (580 mg, 62%). 1H NMR ($DMSO-d_6$) δ 8.83 (s, 1H), 8.03 (d, J = 8.74 Hz, 1H), 7.75 (s, 1H), 6.91 (d, J = 4.68 Hz, 1H), 6.66 (d, J = 2.24 Hz, 1H), 6.51 (dd, J = 2.23, 6.44 Hz, 1H), 3.85 (s, 3H), 3.13 (t, J = 4.54 Hz, 4H), 2.46 (t, J = 4.84 Hz, 4H), 2.22 (s, 3H).

b. Following the general procedure for Suzuki coupling, **13e** and 2-methoxybenzeneboronic acid were converted to **23** as a yellow solid (38 mg, 37% yield). 1H NMR ($DMSO-d_6$) δ 8.88 (s, 1H), 7.83 (t, J = 8.76 Hz, 2H), 7.48 (s, 1H), 7.43 (t, J = 7.16 Hz, 1H), 7.19 (d, J = 8.36 Hz, 1H), 7.08 (t, J = 7.52 Hz, 1H), 6.94 (d, J = 4.68 Hz, 1H), 6.90 (d, J = 4.60 Hz, 1H), 6.63 (s, 1H), 6.35 (d, J = 9.04 Hz, 1H), 3.84 (s, 3H), 3.78 (s, 3H), 3.05–3.16 (broad m, 4H), 2.46 (broad s, 4H), 2.23 (s, 3H). LCMS (ESI^+) m/z 445.19 ($M + H$) $^+$. HPLC: 95 Area%.

(S)-1-(4-{3-Methoxy-4-[7-(2-methoxy-phenyl)-pyrrolo[2,1-f][1,2,4]triazin-2-ylamino]-phenyl}-piperazin-1-yl)-propan-2-ol (**25**) [Method A]. Following the general procedure for S_NAr displacement, **12a** and (S)-1-[4-(4-amino-3-methoxyphenyl)-piperazin-1-yl]-propan-2-ol were converted to **25** as a yellow solid (61 mg, 36%); mp 79–88 °C. 1H NMR ($CDCl_3$) δ 8.67 (s, 1H), 8.24 (d, J = 8.8 Hz, 1H), 8.01 (m, 1H), 7.42 (m, 1H), 7.31 (br s, 1H), 7.12 (m, 1H), 7.06 (d, J = 8.8 Hz, 1H), 7.00 (s, 1H), 6.80 (d, J = 4.7 Hz, 1H), 6.53 (s, 1H), 6.42 (m, 1H), 3.89 (m, 1H), 3.88 (s, 3H), 3.84 (s, 3H), 3.14 (m, 4H), 2.84 (m, 2H), 2.56 (m, 2H), 2.35 (m, 2H), 2.00 (s, 1H), 1.16 (d, J = 7.1 Hz, 3H). LC/MS (ESI^+) m/z 489.22 ($M + H$) $^+$. HPLC: 96 Area%.

(R)-1-(4-{3-Methoxy-4-[7-(2-methoxy-phenyl)-pyrrolo[2,1-f][1,2,4]triazin-2-ylamino]-phenyl}-piperazin-1-yl)-propan-2-ol (**26**) [Method A]. Following the general procedure for S_NAr displacement, **12a** and (R)-1-[4-(4-amino-3-methoxyphenyl)-piperazin-1-yl]-propan-2-ol (synthesized using the exact procedure for the (S) isomer, except (R)-methyloxirane was used) were converted to **26** as a yellow solid (50 mg, 30%); mp 76–85 °C. 1H NMR ($CDCl_3$) δ 8.67 (s, 1H), 8.24 (d, J = 8.8 Hz, 1H), 8.01 (m, 1H), 7.42 (m, 1H), 7.31 (br s, 1H), 7.12 (m, 1H), 7.06 (d, J = 8.8 Hz, 1H), 7.00 (s, 1H), 6.80 (d, J = 4.7 Hz, 1H), 6.53 (s, 1H),

6.42 (m, 1H), 3.89 (m, 1H), 3.88 (s, 3H), 3.84 (s, 3H), 3.14 (m, 4H), 2.84 (m, 2H), 2.56 (m, 2H), 2.35 (m, 2H), 2.00 (s, 1H), 1.16 (d, $J = 7.1$ Hz, 3H). LC/MS (ESI⁺) m/z 489.22 (M + H)⁺. HPLC: 97 Area%.

[2-Methoxy-4-(4-morpholin-4-yl-piperidin-1-yl)-phenyl]-[7-(2-methoxy-phenyl)-pyrrolo[2,1-*f*][1,2,4]triazin-2-yl]-amine (27) [Method A]. Following the general procedure for S_NAr displacement, **12a** and 2-methoxy-4-(4-morpholin-4-yl-piperidin-1-yl)-phenylamine were converted to **27** as the TFA salt (140 mg, 51% yield) as a lyophilized powder. The neutral form could be obtained in quantitative yield by neutralization with aq NaHCO₃ and extraction with dichloromethane or ethyl acetate, followed by drying and concentrating. LC/MS (ESI⁺) m/z 515 (M + H)⁺. TFA salt: ¹H NMR (DMSO-*d*₆) δ 9.90 (broad s, 1H), 8.91 (s, 1H), 7.90 (d, $J = 8$ Hz, 1H), 7.85 (d, $J = 8$ Hz, 1H), 7.56 (s, 1H), 7.45 (t, $J = 7$ Hz, 1H), 7.20 (d, $J = 7$ Hz, 1H), 7.10 (t, $J = 7$ Hz, 1H), 6.95 (q, $J = 5$ Hz, 14 Hz, 2H), 6.73 (s, 1H), 6.46 (d, $J = 7$ Hz, 1H), 4.03 (d, $J = 10$ Hz, 2H), 3.87 (s, 3H), 3.80 (s, 3H), 3.70 (m, 2H), 3.50 (m, 2H), 3.36 (m, 1H), 3.13 (m, 2H), 2.73 (t, $J = 10$ Hz, 2H), 2.16 (d, $J = 10$ Hz, 2H), 2.13 (m, 2H), 1.76 (m, 2H). Neutral form: ¹³C NMR (DMSO-*d*₆) δ 156.8, 152.8, 151.8, 149.4, 147.3, 130.5, 129.7, 126.9, 120.7, 120.6, 120.0, 119.8, 118.8, 114.6, 111.5, 107.1, 105.1, 100.6, 66.5, 61.1, 55.7, 55.4, 49.5, 48.9, 27.7; high resolution mass spectrum m/z 515.2758 [(M + H)⁺ calcd for C₂₉H₃₃N₆O₃ 515.2771]; HPLC: 99 Area%.

{2-Methoxy-4-[4-(4-methyl-piperazin-1-yl)-piperidin-1-yl]-phenyl}-[7-(2-methoxy-phenyl)-pyrrolo[2,1-*f*][1,2,4]triazin-2-yl]-amine (28) [Method A]. Following the general procedure for S_NAr displacement, **12a** and 2-methoxy-4-[4-(4-methyl-piperazin-1-yl)-piperidin-1-yl]-phenylamine were converted to **28** (360 mg, 25%) isolated as a off-white foam. ¹H NMR (DMSO-*d*₆) δ 8.89 (s, 1H), 7.82 (d, $J = 8.9$ Hz, 2H), 7.48 (s, 1H), 7.46–7.41 (m, 1H), 7.20 (d, $J = 8.7$ Hz, 1H), 7.09 (t, $J = 8.0$ Hz, 1H), 6.95 (d, $J = 4.9$ Hz, 1H), 6.90 (d, $J = 4.9$ Hz, 1H), 6.63 (d, $J = 2.4$ Hz, 1H), 6.38–6.35 (m, 1H), 3.84 (s, 3H), 3.79 (s, 3H), 3.65 (broad d, $J = 12.2$ Hz, 2H), 2.67–2.51 (broad m, 6H), 2.37–2.25 (broad absorption, 5H) 2.16 (s, 3H), 1.83 (broad d, $J = 12.9$ Hz, 2H), 1.56–1.46 (m, 2H). LC/MS (ESI⁺) m/z 528 (M + H)⁺. HPLC: 99 Area%.

***N*-[2-{2-[2-Methoxy-4-(4-methyl-piperazin-1-yl)-phenylamino]-pyrrolo[2,1-*f*][1,2,4]triazin-7-yl}-phenyl]-*N*-methyl-methanesulfonamide TFA salt (29) [Method A].** Following the general procedure for S_NAr displacement, *N*-[2-(2-methanesulfinyl-pyrrolo[2,1-*f*][1,2,4]triazin-7-yl)-phenyl]-*N*-methyl-methanesulfonamide and 2-methoxy-4-(4-methyl-piperazin-1-yl)-phenylamine were converted to **29** (28 mg, 17% yield) as a TFA salt pale-yellow powder. ¹H NMR (DMSO-*d*₆) δ 9.65 (broad s, 1H), 8.92 (s, 1H), 7.98 (d, $J = 8$ Hz, 1H), 7.75 (d, $J = 9$ Hz, 1H), 7.64 (m, 2H), 7.53 (m, 2H), 6.96 (q, $J = 5$ Hz, 19 Hz, 2H), 6.71 (s, 1H), 6.43 (d, $J = 9$ Hz, 1H), 3.84 (s, 3H), 3.79 (m, 2H), 3.53 (d, $J = 12$ Hz, 2H), 3.17 (q, $J = 12$ Hz, 2H), 3.08 (s, 3H), 2.93 (m, 2H), 2.88 (m, 6H). LC/MS (ESI⁺) m/z 522 (M + H)⁺. HPLC: 97 Area%.

***N*-[2-{2-[4-((*S*)-2-Hydroxy-propyl)-piperazin-1-yl]-2-methoxy-phenylamino}-pyrrolo[2,1-*f*][1,2,4]triazin-7-yl)-phenyl]-*N*-methyl-methanesulfonamide (30) [Method A].** Following the general procedure for S_NAr displacement, *N*-[2-(2-methanesulfinyl-pyrrolo[2,1-*f*][1,2,4]triazin-7-yl)-phenyl]-*N*-methylmethanesulfonamide and (*S*)-1-[4-(4-amino-3-methoxy-phenyl)-piperazin-1-yl]-propan-2-ol were converted to **30** (1.25 g, 43% yield) as the TFA salt. The neutral form could be obtained in quantitative yield by neutralization with aq NaHCO₃ and extraction with dichloromethane or ethyl acetate, followed by drying and concentrating. LC/MS (ESI⁺) m/z 566 (M + H)⁺. Neutral form: ¹H NMR (DMSO-*d*₆) δ 8.90 (s, 1H), 7.97 (m, 1H), 7.63 (m, 3H), 7.53 (m, 2H), 6.94 (dd, $J = 5$ Hz, 22 Hz, 2H), 6.62 (m, 1H), 6.35 (d, $J = 9$ Hz, 1H), 4.31 (m, 1H), 3.80 (m, 4H), 3.32 (s, 3H), 3.05 (s, 3H), 2.88 (s, 3H), 2.56 (m, 4H), 2.26 (m, 2H), 1.07 (d, $J = 6$ Hz, 3H). TFA salt: ¹³C NMR (DMSO-*d*₆) δ 153.0, 152.0, 150.2, 145.9, 140.1, 131.1, 130.2, 129.3, 121.6, 120.9, 120.7, 117.3, 114.4, 114.4, 111.5, 107.1,

105.5, 100.7, 61.6, 60.5, 55.8, 52.5, 50.0, 45.8, 45.7, 38.3, 36.9, 21.3; high resolution mass spectrum m/z 566.2547 [(M + H)⁺ calcd for C₂₈H₃₆N₇O₄S 566.2549]. HPLC: 96 Area%.

***N*-[2-{2-[4-((*R*)-2-Hydroxy-propyl)-piperazin-1-yl]-2-methoxy-phenylamino}-pyrrolo[2,1-*f*][1,2,4]triazin-7-yl)-phenyl]-*N*-methyl-methanesulfonamide TFA Salt (31) [Method A].** Following the general procedure for S_NAr displacement, *N*-[2-(2-methanesulfinyl-pyrrolo[2,1-*f*][1,2,4]triazin-7-yl)-phenyl]-*N*-methylmethanesulfonamide and (*R*)-1-[4-(4-amino-3-methoxy-phenyl)-piperazin-1-yl]-propan-2-ol were converted to **31** (96 mg, 24% yield) as a TFA salt as a dark-orange powder. ¹H NMR (DMSO-*d*₆) δ 9.48 (br, 1H), 8.93 (s, 1H), 7.97 (m, 1H), 7.75 (d, $J = 8$ Hz, 1H), 7.65 (m, 2H), 7.53 (m, 2H), 6.94 (dd, $J = 5$ Hz, 22 Hz, 2H), 6.70 (m, 1H), 6.43 (d, $J = 9$ Hz, 1H), 4.13 (m, 1H), 3.83 (m, 3H), 3.76 (m, 2H), 3.58 (m, 2H), 3.20 (m, 4H), 3.07 (s, 3H), 3.03 (s, 2H), 2.88 (s, 3H), 1.15 (d, $J = 6$ Hz, 3H). LC/MS (ESI⁺) m/z 566 (M + H)⁺. HPLC: 95 Area%.

***N*-[2-{2-[2-Methoxy-4-(4-morpholin-4-yl-piperidin-1-yl)-phenylamino]-pyrrolo[2,1-*f*][1,2,4]triazin-7-yl)-phenyl]-*N*-methyl-methanesulfonamide (32) [Method A].** Following the general procedure for S_NAr displacement, *N*-[2-(2-methanesulfinyl-pyrrolo[2,1-*f*][1,2,4]triazin-7-yl)-phenyl]-*N*-methylmethanesulfonamide and 2-methoxy-4-(4-morpholin-4-yl-piperidin-1-yl)-phenylamine were converted to **32** (1.50 g, 43% yield) as the TFA salt. The neutral form could be obtained in quantitative yield by neutralization with aq NaHCO₃ and extraction with dichloromethane or ethyl acetate, followed by drying and concentrating. LC/MS (ESI⁺) m/z 592 (M + H). Neutral form: ¹H NMR (DMSO-*d*₆) δ 8.90 (s, 1H), 7.96 (m, 1H), 7.63 (m, 3H), 7.52 (m, 2H), 6.96 (d, $J = 4$ Hz, 1H), 6.91 (d, $J = 4$ Hz, 1H), 6.62 (d, $J = 4$ Hz, 1H), 6.36 (q, $J = 2$ Hz, 8 Hz, 1H), 3.80 (s, 3H), 3.66 (m, 2H), 3.58 (t, $J = 5$ Hz, 4H), 3.32 (m, 4H), 3.05 (s, 3H), 2.88 (s, 3H), 2.62 (m, 2H), 2.25 (m, 1H), 1.86 (m, 2H), 1.50 (m, 2H). TFA salt: ¹³C NMR (DMSO-*d*₆) δ 152.9, 151.9, 150.1, 145.3, 140.1, 131.1, 130.2, 129.3, 121.9, 120.8, 120.7, 117.2, 114.5, 114.3, 111.4, 107.9, 105.6, 101.2, 63.6, 62.4, 55.8, 48.6, 48.4, 38.3, 36.8, 25.3; high resolution mass spectrum m/z 592.2708 [(M + H)⁺ calcd for C₃₀H₃₈N₇O₄S 592.2706]. HPLC: 96 Area%

In Vitro Assays. Enzymatic assays, cellular ALK tyrosine phosphorylation assay, in vitro cytotoxicity assays, and caspase 3/7 assays were reported previously. See ref 10.

In Vivo Assays. Pharmacokinetic assays in the rat and mouse: Sprague–Dawley rats and Scid mice were treated with one dose of compound either iv or orally. At varying time points, blood samples were collected and plasma was obtained. Compound levels in plasma were analyzed and quantitated by LC/MS/MS. Pharmacokinetic parameters were determined with WinNonlin software.

In vivo biochemical efficacy assays (PK/PD study) and tissue distribution studies: Scid mice bearing ALK positive ALCL sc tumors (2 per time point) were treated with vehicle or compound once, po. At appropriate time points, the animals were sacrificed and plasma and tumors were taken and samples prepared. Total and tyrosine phosphorylated NPM-ALK in tumors was measured by immunoblotting. Compound levels in plasma and tumor were analyzed and quantitated by LC/MS.

Antitumor efficacy studies: Tumor bearing mice (8 per group) were treated with compound with the schedule determined from PK/PD studies for a period of 12–17 days (antitumor efficacy study in sc xenograft models). Mice were monitored for signs of morbidity (behavior and body weight loss), and tumors were measured 3 times per week. At the termination of the study, plasma and tumors were harvested and compound levels in the samples measured by LC/MS.

■ ASSOCIATED CONTENT

S Supporting Information. Modeling results for IR and IGF-1R, experimental procedures and analytical data for anilines

used in the synthesis **18**, **25**, **26**, **30**, and **31**. This material is available free of charge via the Internet at <http://pubs.acs.org>.

AUTHOR INFORMATION

Corresponding Author

*Phone: 610-738-6861. Fax: (610)-344-0068. E-mail: gott@cephalon.com.

ACKNOWLEDGMENT

We thank Gervan Williams and Deborah Galinis for performing the Caco-2 permeability assays.

ABBREVIATIONS USED

μ W, microwave; ADME, absorption distribution metabolism excretion; ALCL, anaplastic large-cell lymphoma; ALK, anaplastic lymphoma kinase; ATP, adenosine triphosphate; NPM, nucleophosmin; AUC, area under the curve; bid, bis in die (twice a day); BCR-ABL, breakpoint cluster region-Abelson; CL, intrinsic clearance; C_{max} , maximum concentration; cMet, MNNG HOS (N-methyl-N'-nitro-N-nitrosoguanidine-treated human osteosarcoma) transforming gene; CML, chronic myelogenous leukemia; CYP, cytochrome P450; EGFR, epidermal growth factor receptor; EML4, echinoderm microtubule-associated protein-like 4; F (%), fraction absorbed (oral bioavailability); hERG, human ether-a-go-go related gene; HPLC, high-pressure/performance liquid chromatography; iv, intravenous; IGF-1R, insulin-like growth factor-1 receptor; IR, insulin receptor; KRAS, Kirsten rat sarcoma gene; LC-MS, liquid chromatography–mass spectrometry; Leu, leucine; Met, methionine; NMR, nuclear magnetic resonance; NSCLC, nonsmall cell lung cancer; po, per os (oral); p38 α MAP, P38-alpha mitogen-activated protein; P_{app} , apparent permeability coefficient; PDB, Protein Data Bank; PDR, product distribution ratio (P_{app} , B \rightarrow A/ P_{app} , A \rightarrow B); PEG400, polyethyleneglycol-400; Phe, phenylalanine; PK/PD, pharmacokinetic/pharmacodynamic; S(90), selectivity score 90% inhibition; SAR, structure–activity relationship; siRNA, small interfering RNA; $t_{1/2}$, half-life; TGI, tumor growth inhibition; t_{max} , time of maximum concentration; TP53, tumor promoter 53; Tyr, tyrosine; V_d , volume of distribution; VEGF-R2, vascular endothelial growth factor-receptor 2

REFERENCES

- (1) Gostissa, M.; Alt, F. W.; Chiarle, R. Mechanisms that Promote and Suppress Chromosomal Translocations in Lymphocytes. *Annu. Rev. Immunol.* **2011**, *29*, 319–350.
- (2) Druker, B. J. Imatinib as a paradigm of targeted therapies. *Adv. Cancer Res.* **2004**, *91*, 1–30.
- (3) Deininger, M.; Buchdunger, E.; Druker, B. J. The development of imatinib as a therapeutic agent for chronic myeloid leukemia. *Blood* **2005**, *105*, 2640–2653.
- (4) Chiarle, R.; Voena, C.; Ambrogio, C.; Piva, R.; Inghirami, G. The anaplastic lymphoma kinase in the pathogenesis of cancer. *Nature Rev. Cancer* **2008**, *8* (1), 11–23.
- (5) Webb, T. R.; Slavish, J.; George, R. E.; Look, A. T.; Xue, L.; Jiang, Q.; Cui, X.; Rentrop, W. B.; Morris, S. W. Anaplastic lymphoma kinase: role in cancer pathogenesis and small-molecule inhibitor development for therapy. *Expert Rev. Anticancer Ther.* **2009**, *9* (3), 331–356.
- (6) Chiarle, R.; Gong, J. Z.; Guaspari, I.; Pesci, A.; Cai, J.; Liu, J.; Simmons, W. J.; Dhall, G.; Howes, J.; Piva, R.; Inghirami, G. NPM-ALK transgenic mice spontaneously develop T-cell lymphomas and plasma cell tumors. *Blood* **2003**, *101* (5), 1919–1927.
- (7) Turner, S. D.; Tooze, R.; MacLennan, K.; Alexander, D. R. Vav-promoter regulated oncogenic fusion protein NPM-ALK in transgenic mice causes B-cell lymphomas with hyperactive Jun kinase. *Oncogene* **2003**, *22* (49), 7750–7761.
- (8) Jager, R.; Hahne, J.; Jacob, A.; Egert, A.; Schenkel, J.; Wernert, N.; Schorle, H.; Wellmann, A. Mice transgenic for NPM-ALK develop non-Hodgkin lymphomas. *Anticancer Res.* **2005**, *5*, 3191–3196.
- (9) Piva, R.; Chiarle, R.; Manazza, A. D.; Taulli, R.; Simmons, W.; Ambrogio, C.; D'Escamard, V.; Pellegrino, E.; Ponzetto, C.; Palestro, G.; Inghirami, G. Ablation of oncogenic ALK is a viable therapeutic approach for anaplastic large-cell lymphomas. *Blood* **2006**, *107* (2), 689–697.
- (10) Wan, W.; Albom, M. S.; Lu, L.; Quail, M. R.; Becknell, N. C.; Weinberg, L. R.; Reddy, D. R.; Holskin, B. P.; Angeles, T. S.; Underiner, T. L.; Meyer, S. L.; Hudkins, R. L.; Dorsey, B. D.; Ator, M. A.; Ruggeri, B. A.; Cheng, M. Anaplastic lymphoma kinase activity is essential for the proliferation and survival of anaplastic large-cell lymphoma cells. *Blood* **2006**, *107* (4), 1617–1623.
- (11) Galkin, A. V.; Melnick, J. S.; Kim, S.; Hood, T. L.; Li, N.; Li, L.; Xia, G.; Steensma, R.; Chopiuk, G.; Jiang, J.; Wan, Y.; Ding, P.; Liu, Y.; Sun, F.; Schultz, P. G.; Gray, N. S.; Warmuth, M. Identification of NVP-TAE684, a potent, selective and efficacious inhibitor of NPM-ALK. *Proc. Natl. Acad. Sci. U.S.A.* **2007**, *104*, 270–275.
- (12) Christensen, J. G.; Zou, H.; Arango, M.; Li, Q.; Lee, J. H.; McDonnell, S. R.; Yamazaki, S.; Alton, G.; Mroczkowski, B.; Los, G. Cytoreductive antitumor activity of PF-2341066, a novel Inhibitor of anaplastic lymphoma kinase and c-Met, in experimental models of anaplastic large-cell lymphoma. *Mol. Cancer. Ther.* **2007**, *6*, 3389–3395.
- (13) Soda, M.; Choi, Y. L.; Enomoto, M.; Takada, S.; Yamashita, Y.; Ishikawa, S.; Fujiwara, S.; Watanabe, H.; Kurashina, K.; Hatanaka, H.; Bando, M.; Ohno, S.; Ishikawa, Y.; Aburatani, H.; Niki, T.; Sohara, Y.; Sugiyama, Y.; Mano, H. Identification of the transforming EML4-ALK fusion gene in non-small-cell lung cancer. *Nature* **2007**, *448* (7153), 561–566.
- (14) Rikova, K.; Guo, A.; Qingfu, Z.; Possemato, A.; Yu, J.; Haack, H.; Nardone, J.; Lee, K.; Reeves, C.; Li, Y.; Hu, Y.; Tan, Z.; Stokes, M.; Sullivan, L.; Mitchell, J.; Wetzel, R.; MacNeill, J.; Ren, J. M.; Yuan, J.; Bakalarski, C. E.; Villen, J.; Kornhauser, J. M.; Smith, B.; Li, D.; Zhou, X.; Gygi, S. P.; Gu, T.-L.; Polakiewicz, R. D.; Rush, J.; Comb, M. J. Global survey of phosphotyrosine signaling identifies oncogenic kinases in lung cancer. *Cell* **2007**, *131* (6), 1190–1203.
- (15) Choi, Y. L.; Takeuchi, K.; Soda, M.; Inamura, K.; Togashi, Y.; Hatano, S.; Enomoto, M.; Hamada, T.; Haruta, H.; Watanabe, H.; Kurashina, K.; Hatanaka, H.; Ueno, T.; Takada, S.; Yamashita, Y.; Sugiyama, Y.; Ishikawa, Y.; Mano, H. Identification of novel isoforms of the EML4-ALK transforming gene in non-small cell lung cancer. *Cancer Res.* **2008**, *68* (13), 4971–4976.
- (16) Inamura, K.; Takeuchi, K.; Togashi, Y.; Nomura, K.; Ninomiya, H.; Okui, M.; Satoh, Y.; Okumura, S.; Nakagawa, K.; Soda, M.; Choi, Y. L.; Niki, T.; Mano, H.; Ishikawa, Y. EML4-ALK fusion is linked to histological characteristics in a subset of lung cancers. *J. Thorac. Oncol.* **2008**, *3*, 13–17.
- (17) Wong, D. W.; Leung, E. L.; So, K. K.; Tam, I. Y.; Sihoe, A. D.; Cheng, L. C.; Ho, K. K.; Au, J. S.; Chung, L. P.; Wong, M. The EML4-ALK fusion gene is involved in various histologic types of lung cancers from nonsmokers with wild-type EGFR and KRAS. *Cancer* **2009**, *115* (8), 1723–1733.
- (18) Inamura, K.; Takeuchi, K.; Togashi, Y.; Hatano, S.; Ninomiya, H.; Motoi, N.; Mun, M. Y.; Sakao, Y.; Okumura, S.; Nakagawa, K.; Soda, M.; Choi, Y. L.; Mano, H.; Ishikawa, Y. EML4-ALK lung cancers are characterized by rare other mutations, a TTF-1 cell lineage, an acinar histology, and young onset. *Mod. Pathol.* **2009**, *22* (4), 508–515.
- (19) Soda, M.; Takada, S.; Takeuchi, K.; Choi, Y. L.; Enomoto, M.; Ueno, T.; Haruta, H.; Hamada, T.; Yamashita, Y.; Ishikawa, Y.; Sugiyama, Y.; Mano, H. A mouse model for EML4-ALK positive lung cancer. *Proc. Natl. Acad. Sci. U.S.A.* **2008**, *105*, 19893–19897.
- (20) Mossé, Y. P.; Laudenslager, M.; Longo, L.; Cole, K. A.; Wood, A.; Attiyeh, E. F.; Laquaglia, M. J.; Sennett, R.; Lynch, J. E.; Perri, P.

Laureys, G.; Speleman, F.; Kim, C.; Hou, C.; Hakonarson, H.; Torkamani, A.; Schork, N. J.; Brodeur, G. M.; Tonini, G. P.; Rappaport, E.; Devoto, M.; Maris, J. M. Identification of ALK as a major familial neuroblastoma predisposition gene. *Nature* **2008**, *455* (7215), 930–936.

(21) Chen, Y.; Takita, J.; Choi, Y. L.; Kato, M.; Ohira, M.; Sanada, M.; Wang, L.; Soda, M.; Kikuchi, A.; Igarashi, T.; Nakagawara, A.; Hayashi, Y.; Mano, H.; Ogawa, S. Oncogenic mutations of ALK kinase in neuroblastoma. *Nature* **2008**, *455* (7215), 971–974.

(22) George, R. E.; Sanda, T.; Hanna, M.; Fröhling, S.; Luther, W.; Zhang, J.; Ahn, Y.; Zhou, W.; London, W. B.; McGrady, P.; Xue, L.; Zozulya, S.; Gregor, V. E.; Webb, T. R.; Gray, N. S.; Gilliland, D. G.; Diller, L.; Greulich, H.; Morris, S. W.; Meyerson, M.; Look, A. T. Activating mutations in ALK provide a therapeutic target in neuroblastoma. *Nature* **2008**, *455* (7215), 975–978.

(23) Janoueix-Lerosey, I.; Lequin, D.; Brugières, L.; Ribeiro, A.; de Pontual, L.; Combaret, V.; Raynal, V.; Puisieux, A.; Schleiermacher, G.; Pierron, G.; Valteau-Couanet, D.; Frebourg, T.; Michon, J.; Lyonnet, S.; Amiel, J.; Delattre, O. Somatic and germline activating mutations of the ALK kinase receptor in neuroblastoma. *Nature* **2008**, *455* (7215), 967–970.

(24) Kwak, E. L.; Bang, Y.-J.; Camidge, R.; Shaw, A. T.; Solomon, B.; Maki, R. G.; Ou, S.-H. I.; Dezube, B. J.; Janne, P. A.; Costa, D. B.; Varella-Garcia, M.; Kim, W.-H.; Lynch, T. J.; Fidias, P.; Stubbs, H.; Engelman, J. A.; Sequist, L. V.; Tan, W.; Gandhi, L.; Mino-Kenudson, M.; Wei, G. C.; Shreeve, M.; Ratain, M. J.; Settleman, J.; Christensen, J. G.; Haber, D. A.; Wilner, K.; Salgia, R.; Shapiro, G. I.; Clark, J. W.; Iafrate, A. J. Anaplastic lymphoma kinase inhibition in non-small-cell lung cancer. *New Engl. J. Med.* **2010**, *363*, 1693–1703.

(25) Li, R.; Xue, L.; Zhu, T.; Jiang, Q.; Cui, X.; Yan, Z.; McGee, D.; Wang, J.; Gantla, V. R.; Pickens, J. C.; McGrath, D.; Chucholowski, A.; Morris, S. W.; Webb, T. R. Design and Synthesis of 5-Aryl-pyridone-carboxamides as Inhibitors of Anaplastic Lymphoma Kinase. *J. Med. Chem.* **2006**, *49* (3), 1006–1015.

(26) Sabbatini, P.; Korenchuk, S.; Rowand, J. L.; Groy, A.; Liu, Q.; Leperi, D.; Atkins, C.; Dumble, M.; Yang, J.; Anderson, K.; Kruger, R. G.; Gontarek, R. R.; Maksimchuk, K. R.; Suravajjala, S.; Lapierre, R. R.; Shotwell, J. B.; Wilson, J. W.; Chamberlain, S. D.; Rabindran, S. K.; Kumar, R. GSK1838705A inhibits the insulin-like growth factor-1 receptor and anaplastic lymphoma kinase and shows antitumor activity in experimental models of human cancers. *Mol. Cancer Ther.* **2009**, *8* (10), 2811–2820.

(27) Bossi, R. T.; Saccardo, M. B.; Ardini, E.; Menichincheri, M.; Rusconi, L.; Magnaghi, P.; Orsini, P.; Avanzi, N.; Lombardi Borgia, A.; Nesi, M.; Bandiera, T.; Fogliatto, G.; Bertrand, J. A. Crystal Structures of Anaplastic Lymphoma Kinase in Complex with ATP-Competitive Inhibitors. *Biochemistry* **2010**, *49* (32), 6813–6825.

(28) Deng, X.; Wang, J.; Zhang, J.; Sim, T.; Kim, N. D.; Sasaki, T.; Luther, W., II; George, R. E.; Janne, P. A.; Gray, N. S. Discovery of 3,5-Diamino-1,2,4-triazole Ureas as Potent Anaplastic Lymphoma Kinase Inhibitors. *ACS Med. Chem. Lett.* **2011**, *2*, 379–384.

(29) Sakamoto, H.; Tsukaguchi, T.; Hiroshima, S.; Kodama, T.; Kobayashi, T.; Fukami, T. A.; Oikawa, N.; Tsukuda, T.; Ishii, N.; Aoki, Y. CH5424802, a Selective ALK Inhibitor Capable of Blocking the Resistant Gatekeeper Mutant. *Cancer Cell* **2011**, *19* (5), 679–690.

(30) For recent reviews see ref 5 and Li, R.; Morris, S. W. Development of anaplastic lymphoma kinase (ALK) small-molecule inhibitors for cancer therapy. *Med. Res. Rev.* **2008**, *28* (3), 372–412.

(31) Recently, preclinical evaluation of novel small-molecule ALK inhibitors has been reported, although no structures were disclosed, see: (a) Katayama, R.; Khan, T. M.; Benes, C.; Lifshits, E.; Ebi, H.; Rivera, V. M.; Shakespeare, W. C.; Iafrate, A. J.; Engelman, J. A.; Shaw, A. T. Therapeutic strategies to overcome crizotinib resistance in non-small cell lung cancers harboring the fusion oncogene EML4-ALK. *Proc. Natl. Acad. Sci. U.S.A.* **2011**, *108* (18), 7535–7540. (b) Ardini, E.; Menichincheri, M.; De Ponti, C.; Amboldi, N.; Ballinari, D.; Saccardo, M. B.; Croci, V.; Stellari, F.; Texido, G.; Orsini, P.; Perrone, E.; Bandiera, T.; Borgia, A. L.; Lansen, J.; Isacchi, A.; Colotta, F.; Pesenti, E.; Magnaghi, P.; Galvani, A. A highly potent, selective and orally available ALK inhibitor

with demonstrated antitumor efficacy in ALK dependent lymphoma and non small cell lung cancer models. *Proc. Am. Assoc. Cancer Res.* April, **2009**, Abstract 3737.

(32) Milkiewicz, K. L.; Weinberg, L. R.; Albom, M. S.; Angeles, T. S.; Cheng, M.; Ghose, A. K.; Roemmele, R. C.; Therooff, J. P.; Underiner, T. L.; Zificsak, C. A.; Dorsey, B. D. Synthesis and structure–activity relationships of 1,2,3,4-tetrahydropyrido[2,3-*b*]pyrazines as potent and selective inhibitors of the anaplastic lymphoma kinase. *Bioorg. Med. Chem.* **2010**, *18*, 4351–4362.

(33) Ott, G. R.; Tripathy, R.; Cheng, M.; McHugh, R.; Anzalone, A. V.; Underiner, T. L.; Curry, M. A.; Quail, M. R.; Lu, L.; Wan, W.; Angeles, T. S.; Albom, M. S.; Aimone, L. D.; Ator, M. A.; Ruggeri, B. A.; Dorsey, B. D. Discovery of a Potent Inhibitor of Anaplastic Lymphoma Kinase with in Vivo Antitumor Activity. *ACS Med. Chem. Lett.* **2010**, *1*, 493–498.

(34) Mesaros, E. F.; Burke, J. P.; Parrish, J. D.; Dugan, B. J.; Anzalone, A. V.; Angeles, T. S.; Albom, M. S.; Aimone, L. D.; Quail, M. R.; Wan, W.; Lu, L.; Huang, Z.; Ator, M. A.; Ruggeri, B. A.; Cheng, M.; Ott, G. R.; Dorsey, B. D. Novel 2,3,4,5-tetrahydro-benzo[*d*]azepine derivatives of 2,4-diaminopyrimidine, selective and orally bioavailable ALK inhibitors with antitumor efficacy in ALCL mouse models. *Bioorg. Med. Chem. Lett.* **2011**, *21*, 463–466.

(35) Constraints to form other 6,5-heterocycles have been reported in the kinase literature, see: (a) Choi, H.-S.; Wang, Z.; Richmond, W.; He, X.; Yang, K.; Jiang, T.; Sim, T.; Karanewsky, D.; Gu, X.-J.; Zhou, V.; Liu, Y.; Ohmori, O.; Caldwell, J.; Gray, N.; He, Y. Design and synthesis of 7H-pyrrolo[2,3-*d*]pyrimidines as focal adhesion kinase inhibitors. Part 1, *Bioorg. Med. Chem. Lett.* **2006**, *16*, 2173–2176. (b) Lum, C.; Kahl, J.; Kessler, L.; Kucharski, J.; Lundstrom, J.; Miller, S.; Nakanishi, H.; Pei, Y.; Pryor, K.; Roberts, E.; Sebo, L.; Sullivan, R.; Urban, J.; Wang, Z. 2,5-Diaminopyrimidines and 3,5-disubstituted azapurines as inhibitors of glycogen synthase kinase-3 (GSK-3). *Bioorg. Med. Chem. Lett.* **2008**, *18*, 3578–3581.

(36) Lu, L.; Ghose, A. K.; Quail, M. R.; Albom, M. S.; Durkin, J. T.; Holskin, B. P.; Angeles, T. S.; Meyer, S. L.; Ruggeri, B. A.; Cheng, M. ALK Mutants in the Kinase Domain Exhibit Altered Kinase Activity and Differential Sensitivity to Small Molecule ALK Inhibitors. *Biochemistry* **2009**, *48*, 3600–3609.

(37) Choi, Y. L.; Soda, M.; Yamashita, Y.; Ueno, T.; Takashima, J.; Nakajima, T.; Yatabe, Y.; Takeuchi, K.; Hamada, T.; Haruta, H.; Ishikawa, Y.; Kimura, H.; Mitsudomi, T.; Tanio, Y.; Mano, H. EML4-ALK mutations in lung cancer that confer resistance to ALK inhibitors. *New Engl. J. Med.* **2010**, *363* (18), 1734–1739.

(38) Lee, C. C.; Jia, Y.; Li, N.; Sun, X.; Ng, K.; Ambing, E.; Gao, M.-Y.; Hua, S.; Chen, C.; Kim, S.; Michellys, P.-Y.; Lesley, S. A.; Harris, J.; Spraggon, G. Crystal Structure of the Anaplastic Lymphoma Kinase Catalytic Domain. *Biochem. J.* **2010**, *430*, 425–437; see also ref 27.

(39) Hayashi, M.; Araki, A.; Maeba, I. C-Nucleosides. 17. A synthesis of 2-substituted 7-(β-D-ribofuranosyl)pyrrolo[2,1-*f*]-1,2,4-triazines. A new type of “purine like” C-nucleoside. *Heterocycles* **1992**, *34*, 569–574.

(40) Patil, S. A.; Otter, B. A.; Klein, R. S. 4-Aza-7,9-dideazaadenosine, a new cytotoxic synthetic C-nucleoside analog of adenosine. *Tetrahedron Lett.* **1994**, *35*, 5339–5342.

(41) Hunt, J. T.; Mitt, T.; Borzilleri, R.; Gullo-Brown, J.; Fargnoli, J.; Fink, B.; Han, W.-C.; Mortillo, S.; Vite, G.; Wautlet, B.; Wong, T.; Zheng, X.; Bhide, R. Discovery of the pyrrolo[2,1-*f*][1,2,4]triazine nucleus as a new kinase inhibitor template. *J. Med. Chem.* **2004**, *47*, 4054–4059.

(42) Bhide, R. S.; Cai, Z.-W.; Zhang, Y.-Z.; Qian, L.; Wei, D.; Barbosa, S.; Lombardo, L. J.; Borzilleri, R. M.; Zheng, X.; Wu, L. I.; Barrish, J. C.; Kim, S.-H.; Leavitt, K.; Mathur, A.; Leith, L.; Chao, S.; Wautlet, B.; Mortillo, S.; Jayaseelan, R., Sr.; Kukral, D.; Hunt, J.; Kamath, A.; Fura, A.; Vyas, V.; Marathe, P.; D'Arienzo, C.; Derbin, G.; Fargnoli, J. Discovery and preclinical studies of (R)-1-(4-(4-fluoro-2-methyl-1H-indol-5-yloxy)-5-methylpyrrolo[2,1-*f*][1,2,4]triazin-6-yloxy)propanol (BMS-540215), an in vivo active potent VEGFR-2 inhibitor. *J. Med. Chem.* **2006**, *49*, 2143–2146.

(43) Schroeder, G. M.; Chen, X.-T.; Williams, D. K.; Nirschl, D.; Cai, Z.-W.; Wei, D.; Tokarski, J. S.; An, Y.; Sack, J.; Chen, Z.; Huynh, T.;

Vaccaro, W.; Poss, M.; Wautlet, B.; Gullo-Brown, J.; Kellar, K.; Manne, V.; Hunt, J. T.; Wong, T. W.; Lombardo, L. J.; Fagnoli, J.; Borzilleri, R. M. Identification of pyrrolo[2,1-*f*][1,2,4]triazine-based inhibitors of Met kinase. *Bioorg. Med. Chem. Lett.* **2007**, *18*, 1945–1951.

(44) Wittman, M. D.; Carboni, J. M.; Yang, Z.; Lee, F. Y.; Antman, M.; Attar, R.; Balimane, P.; Chang, C.; Chen, C.; Discenza, L.; Frennesson, D.; Gottardis, M. M.; Greer, A.; Hurlburt, W.; Johnson, W.; Langley, D. R.; Li, A.; Li, J.; Liu, P.; Mastalerz, H.; Mathur, A.; Menard, K.; Patel, K.; Sack, J.; Sang, X.; Saulnier, M.; Smith, D.; Stefanski, K.; Trainor, G.; Velaparthi, U.; Zhang, G.; Zimmermann, K.; Vyas, D. M. Discovery of a 2,4-Disubstituted Pyrrolo[1,2-*f*]-[1,2,4]triazine Inhibitor (BMS-754807) of Insulin-like Growth Factor Receptor (IGF-1R) Kinase in Clinical Development. *J. Med. Chem.* **2009**, *52*, 7360–7363.

(45) For full synthetic procedures for the synthesis of **11** and **15** see: Thieu, T.; Sclafani, J. A.; Levy, D. V.; McLean, A.; Breslin, H. J.; Ott, G. R.; Bakale, R.; Dorsey, B. D. Discovery and Process Synthesis of Novel 2,7-Pyrrolo[2,1-*f*][1,2,4]triazines. *Org. Lett.* **2011**, *13*, 4204–4207.

(46) Mulvihill, M. J.; Ji, Q.-S.; Coate, H. R.; Cooke, A.; Dong, H.; Feng, L.; Foreman, K.; Rosenfeld-Franklin, M.; Honda, A.; Mak, G.; Mulvihill, K. M.; Nigro, A. I.; O'Connor, M.; Pirrit, C.; Steinig, A. G.; Siu, K.; Stolz, K. M.; Sun, Y.; Tavares, P. A. R.; Yao, Y.; Gibson, N. W. Novel 2-phenylquinolin-7-yl-derived imidazo[1,5-*a*]pyrazines as potent insulin-like growth factor-I receptor (IGF-1R) inhibitors. *Bioorg. Med. Chem.* **2008**, *16*, 1359–1375.

(47) Zifcsak, C. A.; Therooff, J. P.; Aimone, L. D.; Albom, M. S.; Angeles, T. S.; Cheng, M.; Mesaros, E. F.; Ott, G. R.; Quail, M. R.; Underiner, T. L.; Wan, W.; Dorsey, B. D. Methanesulfonamido-cyclohexylamine derivatives of 2,4-diaminopyrimidine as potent ALK inhibitors. *Bioorg. Med. Chem. Lett.* **2011**, *21*, 3877–3880.

(48) Selectivity score for 90% inhibition from single point data tested at 1 μ M screening concentration, $S(90)$ = no. of kinases \geq 90% inhibition/total no. of kinases tested.